University of Alberta

Mapping of CYP3A Activity Along the Intestinal Mucosa in Dogs

by

Agatha HoYan Ching

A thesis submitted to the Faculty of Graduate Studies and Research in partial fulfillment of the requirements for the degree of Master of Science

in

Pharmaceutical Sciences

Faculty of Pharmacy and Pharmaceutical Sciences

Edmonton, Alberta

Fall 2000

National Library of Canada
Acquisitions and Bibliographic Services
395 Wellington Street
Ottawa ON K1A 0N4
Canada

Bibliothèque nationale du Canada
Acquisitions et services bibliographiques
395, rue Wellington
Ottawa ON K1A 0N4
Canada

Your file Votre référence

Our file Notre référence

The author has granted a non-exclusive licence allowing the National Library of Canada to reproduce, loan, distribute or sell copies of this thesis in microform, paper or electronic formats.

L'auteur a accordé une licence non exclusive permettant à la Bibliothèque nationale du Canada de reproduire, prêter, distribuer ou vendre des copies de cette thèse sous la forme de microfiche/film, de reproduction sur papier ou sur format électronique.

The author retains ownership of the copyright in this thesis. Neither the thesis nor substantial extracts from it may be printed or otherwise reproduced without the author's permission.

L'auteur conserve la propriété du droit d'auteur qui protège cette thèse. Ni la thèse ni des extraits substantiels de celle-ci ne doivent être imprimés ou autrement reproduits sans son autorisation.

0-612-59790-3

Canada

University of Alberta

Library Release Form

Name of Author: Agatha HoYan Ching

Title of Thesis: Mapping of CYP3A Activity Along the Intestinal Mucosa in Dogs

Degree: Master of Science

Year this Degree Granted: 2000

Permission is hereby granted to the University of Alberta Library to reproduce single copies of this thesis and to lend or sell such copies for private, scholarly, or scientific research purposes only.

The author reserves all other publication and other rights in association with the copyright in the thesis, and except as hereinbefore provided, neither the thesis nor any substantial portion thereof may be printed or otherwise reproduced in any material form whatever without the author's prior written permission.

146 Healy Road,
Edmonton, Alberta
Canada T6R 1V9

Date: Aug 29, 00

ABSTRACT

The current project is undertaken to quantify the activity of CYP3A along the entire length of dogs' small intestines. Intestinal microsomes were prepared from consecutive 1-foot section of four female mongrel dogs' small intestines. For three of four intestines, CYP3A catalytic activity decreased from duodenum to middle jejunum and then increased in middle jejunum and declined thereafter to ileum. CYP3A activity between sections of an intestine ranged from 3-fold to 10-fold. Average (± SD) V_{max} values were 157 (± 56.31), 89 (± 20.22), 54.3 (± 30.14) pmol/min/mg microsomal protein for duodenum, jejunum and ileum, respectively. ANOVA revealed a statistically significant difference in V_{max} between duodenum and ileum (p = 0.0045) and duodenum and jejunum (p = 0.0346), but not between jejunum and ileum (p = 0.2357). Our findings suggest that CYP3A activity is highest in duodenum and lower in jejunum and ileum in dogs' small intestines.

University of Alberta

Faculty of Graduate Studies and Research

The undersigned certify that they have read, and recommend to the Faculty of Graduate Studies and Research for acceptance, a thesis entitled "Mapping of CYP3A Activity Along the Intestinal Mucosa in Dogs" submitted by Agatha Ho Yan Ching in partial fulfillment of the requirements for the degree of Master of Science in Pharmaceutical Sciences.

Dr. Y. K. Tam, Supervisor

Dr. R. T. Coutts

Dr. J. Samuel

Dr. G. Baker

Date: Aug 29, 00

DEDICATION

This thesis is dedicated to:

My God: Jesus Christ

My father: Clement Ching

My mother: Winnie Kwan

My fiancé: Caly Chien

for their love, support and encouragement.

ACKNOWLEDGEMENTS

The author would like to express deep gratitude to Dr. Yun K. Tam for his expert and patient guidance through a most challenging project. His support and understanding through all these years is greatly appreciated. It was a privilege to work under his supervision.

The author sincerely thanks Dr. M. Ma, Dr. J. Jiang and Dr. Xing-Fang Li at Kinetana Inc. for their valuable advice on HPLC assay development and interpretation of the spectra.

TABLE OF CONTENTS

1. INTRODUCTION....1

1.1 Anatomy and circulation of the small intestine....1

1.1.1 Mucosal blood flow....3

1.1.2 Countercurrent exchange....6

1.2 Drug metabolism....8

1.2.1 Cytochrome P450....10

1.2.1.1 The CYP1A family....11

1.2.1.2 The CYP2 family....12

1.2.1.3 The CYP3 family....13

1.3 Localization of drug-metabolizing enzymes in the small intestine....14

1.4 Enzyme kinetics....20

1.5 Intestinal organ clearance....21

1.6 Tissue homogenates and subcellular fractions (S9/microsomes)....26

1.7 High-performance liquid chromatographic method for the separation of testosterone metabolites....26

1.8 Rationale for choosing the dog as an animal model....27

1.9 Hypothesis....29

1.10 Objectives....30

2. EXPERIMENTAL SECTION....31

2.1 Materials and chemical reagents....31

2.2 *In vitro* studies using dog intestines....31

2.2.1 Animals....31

2.2.2 Organ Procurement....32
2.2.3 Preparation of intestinal microsomes....32
2.2.4 Determination of microsomal protein content....33
2.2.5 Incubation studies....34
2.2.6 Instrumentation and chromatographic conditions....35
2.2.7 Standard solution....35
2.2.8 Sample preparation....36
2.2.9 Enzyme kinetics analysis....36
2.2.10 Statistical analysis....37
3. RESULTS....38
3.1 Method development....38
3.2 Precision and accuracy of HPLC method....38
3.3 Extraction recovery....39
3.4 Inter-day precision of determination of enzymatic activities....39
3.5 Distribution of intestinal CYP3A activities....39
3.6 Testosterone 6β-hydroxylation kinetics....40
4. DISCUSSION....58
4.1 Distribution of intestinal CYP3A activities....58
4.2 Testosterone 6β-hydroxylation kinetics....59
5. CONCLUSIONS....63
6. REFERENCES....64

LIST OF TABLES

Table 3.1 Precision and accuracy of 6β-hydroxytestosterone calibration standards.42

Table 3.2 Inter-day precision of determination of enzymatic activities in dog intestine microsomes.....43

Table 3.3 Kinetic parameters for the formation of 6β-hydroxytestosterone in dog intestinal microsomes.....44

LIST OF FIGURES

Figure 1.1 Microcirculation of a human villus.....7

Figure 1.2 Metabolic pathways of testosterone.....28

Figure 3.1 Representative chromatogram of blank microsomes spiked with testosterone, its five metabolites and internal standard. (7α: 7α-hydroxy-testosterone, 6β: 6β-hydroxytestosterone, 16α: 16α-hydroxytestosterone, 16β-hydroxytestosterone, 2α: 2α-hydroxytestosterone, IS: Cortexolone) 45

Figure 3.2 A representative chromatogram of a testosterone sample spiked with internal standard after 10 minutes of incubation with dog intestinal microsomes.....46

Figure 3.3 Calibration curve for 6β-hydroxytestosterone using the internal standard method.....47

Figure 3.4 A typical diagram showing that the UV spectrum (190 - 300 nm) of the 6β-hydroxytestosterone peak in a dog intestine microsome sample (- - -) is superimposable on that of authentic 6β-hydroxytestosterone (------).....48

Figure 3.5 Effect of substrate concentration on the rates of 6β-hydroxylation of testosterone.....49

Figure 3.6 Longitudinal testosterone 6β-hydroxylation rates (at 500 mM testosterone) for dog #1's small intestine.....50

Figure 3.7 Longitudinal testosterone 6β-hydroxylation rates (at 500 mM testosterone) for dog #2's small intestine.....51

Figure 3.8 Longitudinal testosterone 6β-hydroxylation rates (at 500 mM testosterone) for dog #3's small intestine.....52

Figure 3.9 Longitudinal testosterone 6β-hydroxylation rates (at 500 mM testosterone) for dog #4's small intestine.....53

Figure 3.10 Representative Eadie-Hofstee plot of 6β-hydroxytestosterone formation in dog intestine microsomes.....54

Figure 3.11 Average K_m values for duodenum, jejunum and ileum of four dogs' small intestines. ANOVA revealed no differences in K_m values among the three tissues ($p = 0.72$).....55

Figure 3.12 Average V_{max} values for duodenum, jejunum and ileum of four dogs' small intestines. ANOVA revealed a statistically significant difference in V_{max} between duodenum and ileum ($p = 0.0045$) and duodenum and jejunum ($p = 0.0346$), but not between jejunum and ileum ($p = 0.2357$).....56

Figure 3.13 Average CL_{int} values for duodenum, jejunum and ileum of four dogs' small intestines. ANOVA revealed a statistically significant difference in $Cl_{int,mic}$ between duodenum and ileum ($p = 0.0045$) and duodenum and jejunum ($p = 0.0217$), but not between jejunum and ileum ($p = 0.3480$).....57

GLOSSARY OF ABBREVIATIONS AND SYMBOLS

°C	degree Celsius
%	percent
Σ	summation
ANOVA	analysis of variance
ACS	American Chemical Society
AUC	area under the plasma concentration *vs* time curve from time 0 to ∞
C_{in}	drug concentration in the inflow
C_{out}	drug concentration in the outflow
CL_{abs}	intestinal absorption clearance
CL_G	intestinal clearance
CL_H	hepatic clearance
$CL_{int, mic}$	microsomal intrinsic clearance
CL_{int}	intrinsic clearance
$CL_{int, g}$	intestinal intrinsic clearance
$CL_{int, h}$	hepatic intrinsic clearance
CL_{organ}	organ clearance
cm	centimeter(s)
C_{max}	peak concentration
CYP	cytochrome P450
DNA	deoxyribonucleic acid
E	unoccupied enzyme concentration
E	extraction ratio

EDTA	ethylenediaminetetraacetic acid
E_G	intestinal extraction ratio
E_H	hepatic extraction ratio
ES	complexed enzyme concentration
F	bioavailability
f_B	unbound fraction of drug in the blood
G	gauge
h	hour(s)
HPLC	high performance liquid chromatography
i.v.	intravenous
k_1	kinetic constant for substrate-enzyme affinity
k_{-1}	kinetic constant for dissociation of the ES complex
k_{cat}	rate constant for product formation
kg	kilogram(s)
K_m	Michaelis constant
L	liter(s)
m	meter(s)
M	molar
mg	milligram(s)
min	minute(s)
mM	millimolar
µL	microliter(s)
µm	micron(s)

μM	micromolar
MDR	multidrug resistance gene
ml	milliliter(s)
mm	millimeter(s)
mRNA	messenger ribonucleic acid
n	number of observations
NADPH	β-nicotinamide adenine dinucleotide phosphate
ng	nanogram(s)
nm	nanometer(s)
nmol	nanomole
P	product concentration
p	probability of rejecting the null hypothesis when it is true
P-450	cytochrome P450
pH	negative logarithm of concentration of H^+ ions
pmol	picomole
PMSF	phenylmethylsulfonylfluoride
Q	blood flow to the organ
Q_g	mucosal blood flow
Q_h	liver blood flow
r	coefficient of linear relation
S	substrate concentration
SD	standard deviation
SSRI	selective serotonin reuptake inhibitor

T_{max}	time to maximum (peak) concentration
UV	ultra-violet
V_{max}	maximum velocity
v	rate of product formation
v/v	volume per volume

1. INTRODUCTION

1.1 Anatomy and circulation of the small intestine

The small intestine is divided arbitrarily into three parts: duodenum, jejunum, and ileum. There is no sharp distinction among them, but they are slightly different in their absorptive and secretory capabilities. The duodenum is the shortest, widest, and least mobile section in human. It measures 20 to 30 cm in length and 3 to 5 cm in diameter. The rest of the small intestine is about 5 m long; the proximal two-fifths is referred to as the jejunum and the distal three-fifths is called the ileum (Lin *et al*, 1999). The ileum tends to be thinner and narrower, with more mesenteric fat and a more complex pattern of arterial arcades than jejunum. In general, there is a gradual narrowing of the lumen of the small intestine from the proximal duodenum to the distal ileum (Thomas, 1988; Shiner, 1995).

The three regions of the small intestine share a common histological pattern. Their wall, from inside outward, is composed of the mucosa, the submucosa, the muscle layers, and the serosa (Thomas, 1988; Shiner, 1995). The serosa is an extension of the peritoneum and consists of a single layer of flattened mesothelial cells overlying some loose connective tissues. The muscularis is composed of an inner circular and outer longitudinal layer of smooth muscle. The submucosa is a layer of collagenous connective tissue containing hematic and lymphatic vessels as well as nerves that pass into the mucosa. The mucosa has three components; a superficial lining of

epithelium, the lamina propria, and the muscularis mucosa. The epithelium, the innermost layer of mucosa facing the lumen of the bowel, consists of a single layer of columnar epithelial cells (enterocytes) which line both the crypts and the villi. The villi tend to be short and leaf-like in the duodenum and are tall and broader in the jejunum, where their height ranges from 300 to 780 μm. The villus height decreases from the jejunum to the ileum. The total mucosa thickness varies from 530 to 900 μm (Thomas, 1988; Shiner, 1995).

Unlike hepatocytes which regenerate only when untimely death occurs, epithelial cells of intestinal mucosa have a programmed limited life span. The villous epithelial cells are functionally mature and nondividing, whereas the crypt cells are undifferentiated and actively proliferate. The crypt cells continue to mature as they migrate up the wall of the crypt to the base of the villi. Their death rate is estimated at 1 or 2 cells per 100 cells per h. The time required for migration from the base to the tip has been estimated to be 2 to 6 days (Bertalanffy and Nagy, 1961; Lipkin *et al.*, 1963; Creamer, 1967). The following example describes one of the consequence of this rapid migration. Intestinal CYP3A4 enzymes have been shown to activate dietary aflatoxin B_1 to reactive metabolites that form macromolecular adducts within enterocytes (Kolars *et al.*, 1994). Consequently, these adducts should pass harmlessly in stool as the enterocytes are shed as a result of rapid migration. The rapidity of enterocyte migration and maturation may provide a protective mechanism against carcinogenic toxins (Morse and Stoner, 1993; Zhang *et al.*, 1997).

1.1.1 Mucosal Blood Flow

The blood (500 ml/min) that courses through the human small intestine flows immediately into the liver by way of the portal vein. The blood then passes through the hepatocytes in the liver and leaves the liver *via* hepatic veins. The superior mesenteric arteries supply the small intestine by way of an arching arterial system (Lin *et al,* 1999). Blood flowing through a small artery is distributed in the various layers of the small intestine. In dogs, approximately three-fourths of total resting intestinal blood flow is distributed to the mucosa and the remainder to the submucosa, muscularis, and serosa (Bond and Levitt, 1979; Bond *et al.*, 1979). It has also been demonstrated that approximately 60 to 70 % of the intestinal blood flow is distributed to the epithelial mucosal cells of cats and rats (Biber *et al.*, 1973; Gore and Bohlen, 1977). Because only part of the intestinal blood flow reaches the mucosa, the mucosal blood flow, rather than the total intestinal blood flow, should be used when attempts are made to estimate intestinal clearance and extraction (Klippert *et al.*, 1982).

The blood flow in each region of the small intestine, as well as in each layer of the gut wall, is related directly to the metabolic demands of the cells within each region and to the functional activity. During the absorption phase, blood flow in the villi and adjacent regions of the submucosa is increased greatly, whereas blood flow in the muscle layers of the gut wall increases with increased motor activity (Lin *et al,* 1999). After a meal, blood flow increases by 30 to 130 % of basal flow, and the hyperemia is confined to the segment of intestine exposed to the chyme. Long-chain fatty acids

and glucose are the major stimuli for hyperemia, which is likely mediated by hormones such as cholecystokinin released from mucosal endocrine cells (Bond *et al.*, 1979). In addition, there are a number of factors, operating via neurohormonal and local regulatory mechanisms, which can increase the mucosal blood flow in the small intestine (Bond *et al.*, 1979). Sympathetic stimulation, in contrast, decreases the intestinal blood flow by causing intense vasoconstriction of the blood vessels. During heavy exercise, sympathetic vasoconstriction can shut off the intestinal blood flow for short periods of time when increased flow is needed by the skeletal muscle and heart. The effect of exercise on the absorption of midazolam has been investigated in healthy volunteers following a 15-mg oral dose of midazolam (Strömberg *et al.*, 1992). The rate, but not the extent of midazolam absorption, was affected by exercises (treadmill running for 50 min). The C_{max} was decreased from 112 ng/ml in the exercise session, while the T_{max} was increased from 73 to 123 min. However, the AUC was not affected significantly by exercise. The alterations in the absorption of midazolam during exercise are likely attributed to a transitory decrease of mucosal blood flow.

After a meal, blood flow to the small intestine is increased, and as a consequence, hepatic blood flow also is increased. The greater the blood flow, the lower will be the hepatic and intestinal first-pass metabolism, resulting in an increased bioavailability. Hepatic bioavailability (F_H) can be calculated as follows:

$$F_H = 1 - E_H = 1 - \frac{f_B \bullet CL_{int,h}}{Q_h + f_B \bullet CL_{int,h}}$$

$$F_H = \frac{Q_h}{Q_h + f_B \bullet CL_{int,h}}$$

For a drug that exhibits significant first-pass metabolism (*i.e.* a drug with high extraction ratio), $f_B \bullet CL_{int,h} >>> Q_h$. Therefore, the above equation reduces to:

$$F_H = \frac{Q_h}{f_B \bullet CL_{int,h}}$$

Thus an increase of Q_h will increase F_H. Clinical studies demonstrate convincingly that the bioavailability of drugs subject to significant first-pass metabolism during absorption is increased after a meal (Melander and McLean, 1983; Olanoff *et al.*, 1986). A standardized breakfast increased the bioavailability of propranolol and metoprolol by 40 to 50 % in normal volunteers (Melander *et al.*, 1977b). However, the blood flow change is not the sole cause responsible for the increased bioavailability after a meal. For example, it is difficult to explain how a standardized breakfast could increase the bioavailability of hydralazine 2- to 3-fold (Melander *et al.*, 1977a). Other factors, such as food-induced inhibition of hepatic and intestinal drug metabolizing enzymes, also may be involved in the increased bioavailability.

1.1.2 Countercurrent Exchange

The villus is supplied by arterioles that pass to the tip of the villus where they break up into many small capillaries, which then drain into a villus venule (Fig.1.1). Because of the close proximity between the arterioles and venules in the intestinal villi, it is possible that some small molecules can diffuse out from the ascending arterioles directly into the adjacent descending venules without ever being carried in the blood to the tip of the villus where the majority of the intestinal drug-metabolizing enzymes are located (Lin *et al,* 1999). Studies in animals and humans support the concept of countercurrent exchange in the villi (Hallback *et al.*, 1978; Parks and Jacobson, 1987). Because of this exchange phenomenon, the fraction of a drug metabolized by the small intestine could be quantitatively less important when the drug is delivered from the systemic circulation after i.v. administration or the postabsorptive phases as compared to that which occurs during the absorptive phase. In other words, countercurrent exchange reduces the entry of drugs from the systemic circulation into enterocytes. Thus, the presence of this countercurrent is an important feature in intestinal drug metabolism.

Countercurrent exchange is probably accomplished mainly *via* simple diffusion created by a concentration gradient. The effect of countercurrent exchange may vary among substrates depending on their physicochemical properties, as exemplified by the absorption of four diffusible gases (H_2, He, CH_4, and ^{133}Xe) from the small intestine in dogs (Bond *et al.*, 1977). Although these gases were absorbed efficiently from the intestinal lumen (99.7%, 99.9%, 75.6%, 36% of the dose for H_2, He, CH_4,

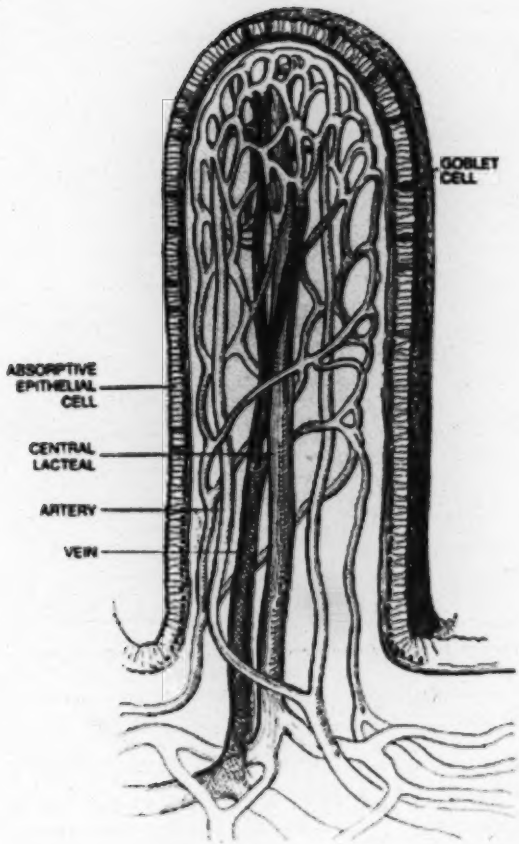

Figure 1.1 Microcirculation of a human villus.

and ^{133}Xe, respectively), the absorbed fraction escaping into the systemic blood circulation was only 16.2%, 12.8%, 12.0%, and 15.8%, respectively, indicating a substantial countercurrent exchange (83.8%, 87.2%, 84.1%, and 56.1%) of the initially absorbed H_2, He, CH_4, and ^{133}Xe.

The effect of countercurrent exchange on the intestinal absorption and metabolism of drugs has not yet been investigated. However, Minchin and Ilett (1982) have incorporated the concept of countercurrent exchange into their pharmacokinetic models for the estimation of the intestinal metabolism of drugs. A proportionality constant (α) relating intestinal metabolism after i.v. administration to that after oral administration was proposed to reflect the back-diffusion (countercurrent exchange) of drugs from the intestinal circulation. Theoretically, α can vary from 0 to 1 depending on the physicochemical properties of a given drug. If a compound is not subject to countercurrent exchange, α will be equal to unity. This means that intestinal metabolism of the drug is similar after i.v. and oral administration (Minchin and Ilett, 1982).

1.2 Drug Metabolism

Drug metabolism is the chemical modification of a drug in a biologic environment. Most drugs undergo metabolic modification in the body, and normally drug metabolism is enzymatically controlled by the actions of oxidases, reductases, esterases, and enzymes involved in conjugation reactions. Drug metabolism occurs in

the liver, kidney, blood, brain, lungs, gastrointestinal tract, skin, and other tissues. The principal function of drug metabolism in the body is to convert drugs to products (metabolites) that are less pharmacologically active and much more water- soluble (i.e. more polar or ionized) than the parent drug and therefore more readily and rapidly excreted. Although it is true that most metabolites are less active pharmacologically and more polar than the parent drug, there are many exceptions to this generalization. "Active metabolites" may possess a pharmacological activity equal to, greater than, or different from, that of the parent drug itself or may contribute significantly to adverse effects. Occasionally, a metabolite is more lipophilic than the drug from which it was formed. For example, the acetylation of such drugs as sulfanilamide, sulfadiazine, and sulfisoxazole produces metabolites that are less water soluble and that in sufficient concentration will precipitate in the kidney tubules, causing kidney damage and crystaluria.

Drug metabolism reactions are classified as phase I or phase II reactions (Gibson and Skett, 1994). A phase I metabolic reaction is one in which a new chemical group is introduced into a drug molecule, especially by oxidative, reductive, and hydrolytic methods. A phase II metabolic reaction is one in which a drug or phase I metabolite is conjugated by an enzymatic process with a small endogenous molecule. Numerous examples of phase I metabolic reactions have been observed and many are oxidative reactions. The primary mechanism by which oxygen is introduced into a molecule is complex, and the reaction is catalyzed by the mixed function oxidases of the endoplasmic reticulum of the liver and other tissues. This has been referred to as the P450 system (consisting of cytochrome P450, cytochrome P450 reductase, and

cytochrome *c* reductase), which requires molecular oxygen and NADPH (or NADP) for the introduction of one atom of oxygen into the drug.

Phase I metabolic reactions include aromatic and aliphatic ring oxidation and N- or O-dealkylation. Phase II metabolic reactions are conjugation reactions of drugs and drug metabolites of the general formula R-XH, where X = NH, NR, O, or S. Most examples of Phase II reactions involve compounds of structure R-OH. Metabolic conjugation reactions that have been observed include (1) conjugation with glucuronic acid, (2) sulfate, (3) acetate, (4) glycine, (5) glutamine and (6) glutathione and (7) methylation. Of these reactions, conjugation with glucuronic acid (which yields a glucuronide) is the most important in humans.

1.2.1 Cytochrome P450

The cytochromes P-450 are the principle enzymes involved in the biotransformation of drugs and other foreign compounds. They comprise a superfamily of hemeproteins that contain a single-iron protoporphyrin IX prosthetic group. This superfamily is subdivided into families and subfamilies that are classified solely on the basis of amino acid sequence homology. To date, at least 14 P-450 gene families have been identified in mammals (Nelson *et al.*, 1996). However, only three main P-450 gene families, *CYP1, CYP2, and CYP3* currently are thought to be responsible for drug metabolism. Approximately 70% of human liver P-450 is accounted for by the CYP1A2, 2A6, 2B6, 2C, 2D6, 2E1, and 3A isoforms. Among these, CYP3A (CYP3A4 and 3A5) and CYP2C (CYP2C8, 2C9, 2C18 and 2C19) are

the most abundant subfamilies, accounting for 30% and 20% of total P-450, respectively (Guengerich, 1995).

1.2.1.1 The CYP1A family

The CYP1 family (Wrighton *et al.*, 1992) is characterized by two genes and is mainly involved in the metabolism of polycyclic aromatic compounds and arylamines. CYP1A1 (aryl hydrocarbon hydroxylase) is found in low concentrations in the liver and extrahepatic tissues such as the lungs. It is induced by polycyclic hydrocarbons. (Wrighton *et al., 1992*) The mechanism of induction in the liver has been studied extensively. Inducing agents diffuse into the liver cells where they bind to the receptors of carrier proteins. The carrier protein complex enters the nucleus where it associates with DNA and stimulates the transcription of mRNA, which leaves the nucleus and promotes the formation of the cytochrome enzyme at the rough endoplasmic reticulum.

CYP1A2 (arylamine oxidations) is important for demethylation of methylxanthines such as caffeine and theophylline, O-demethylation of naproxen, hydroxylation of tacrine, R-warfarin and caffeine, dealkylation of phenacetin and demethylation of the tricyclic antidepressants (Slaughter *et al.*, 1995). The enzyme may be induced by cigarette smoking, charbroiled meat, phenytoin, phenobarbitone and omeprazole. Quinolone antibiotics such as erythromycin and ciprofloxacin inhibit CYP1A2 by the binding of the 4-oxo-carboxylic acid portion of quinolone to

the enzyme (Murray *et al.*, 1992) Fluvoxamine (Nemeroff *et al.*, 1996), a selective serotonin reuptake inhibitor (SSRI), also inhibits CYP1A2.

1.2.1.2 The CYP2 family

This is a large family (Wrighton *et al.*, 1992) that includes 2A, 2B, 2C, 2D and 2E subfamilies. The human 2A subfamily has not been extensively studied. CYP2A6 is an important liver enzyme that hydroxylates coumarin compounds (Wrighton *et al.*, 1992). The role of the 2B subfamily in human liver drug metabolism is limited.

The CYP2C subfamily of enzymes demethylates diazepam and tricyclic antidepressants (amitriptyline, imipramine) and oxidizes omeprazole. Some 2C9 substrates are phenytoin, tolbutamide and diclofenac. 2C10 enzyme is involved in the hydroxylation of tolbutamide and hexobarbitone (Wrighton *et al.*, 1992). These two 2C enzymes are inhibited by sulfaphenazole and sulfinpyrazone. The 2C19 isoform is involved in the metabolism of hexobarbitone, diazepam and S-mephenytoin.

The 2D6 (debrisoquine hydroxylase) enzyme (Kerremans *et al.*, 1996) has been investigated intensively and is involved in the metabolism of a large number of drugs such as debrisoquine, tricyclic antidepressants, selective serotonin reuptake inhibitors (Nemeroff *et al.*, 1996) (except fluvoxamine), analgesics (codeine, dextromethorphan), anti-arrhythmics (encainide, flecanide), β-blockers (metoprolol) and ondansetron. The activity of the CYP2D6 enzyme exhibits a bimodal distribution, indicating the presence of dominant and recessive alleles in the

population (Rowland *et al.*, 1995). This isoenzyme is not inducible by pharmacological agents. Quinidine and the selective serotonin reuptake inhibitors (SSRIs) bind tightly and inhibit the enzyme (Murray *et al.*, 1992). Quinidine effectively changes patients taking drugs which are metabolized by CYP2D6 into poor metabolizers. The SSRIs such as paroxetine and fluoxetine are potent competitive and reversible inhibitors whilst sertraline and fluvoxamine do so to a lesser extent (Nemeroff *et al.*, 1996).

The CYP2E subfamily contains only one gene and is toxicologically an important enzyme (Lieber *et al.*, 1997 and Koop *et al.*, 1992). The CYP2E (dimethylnitrosamine N-demethylase) enzyme is responsible for the metabolism of many volatile anesthetic agents (Kharasch *et al.*, 1995) (such as enflurane, isoflurane, methoxyflurane, diethyl ether and chloroform), ethanol and aromatic compounds such as benzene and paracetamol. The enzymes can be induced by isoniazid and ethanol and inhibited by disulfiram. Chronic ethanol consumption increases the rate of metabolism of pentobarbitone, tolbutamide, propanolol and rifampicin as a result of induction of CYP2E1. In contrast, acute ethanol consumption may competitively inhibit 2E1 and decrease the metabolism of benzodiazepines, phenothiazines, barbiturates, morphine and warfarin.

1.2.1.3 The CYP3 family

The CYP3 family is involved in the metabolism of a large number of endogenous and exogenous compounds and may be induced by steroids, macrolide antibiotics,

antifungal drugs and phenobarbitone (Wrighton *et al.*, 1992). Endogenous compounds metabolized by the 3A subfamily include progesterone, estradiol, cortisol, testosterone and androstenedione. Exogenous compounds that are metabolized by these enzymes include erythromycin, midazolam, alfentanil, cyclosporine and nifedipine (Kerremans *et al.*, 1996). The major pathways for these substrates include oxidation, dealkylation, nitro-reduction and hydroxylation. These enzymes account for about 30% of the hepatic and 70% of the gut wall P450 content (Lieber *et al.*, 1997). This subfamily in humans is controlled by four genes, *CYP 3A3, 3A4, 3A5, 3A7*. The CYP3A4 is the most common and abundant cytochrome subfamily in the liver. CYP3A4 is the main catalyst for the oxidation of fentanyl to norfentanyl in humans (Kharasch *et al.*, 1993); in rats it is 3A1/2. A significant first-pass oxidation of midazolam is brought about by mucosal CYP3A4 of the small intestine (Paine *et al.*, 1996). CYP3A7 is only found in fetal liver. Rifampicin is the most potent inducer of CYP3A enzymes. Other inducers of CYP3A are phenobarbitone and phenytoin. The enzyme is inhibited by ketoconazole, erythromycin, cimetidine and grapefruit juice.

1.3 Localization of drug-metabolizing enzymes in the small intestine

Numerous phase 1 and phase 2 metabolic reactions occur in the gut wall. Almost all of the drug-metabolizing enzymes present in the liver are also found in the small intestine, although their levels are generally much lower in the latter than in the

former. Kinetically, the content of a particular catalytic enzyme within the enterocytes and the intracellular residence time of the drug subject to biotransformation determine the rate of intestinal metabolism of a drug. It is, therefore, important to determine the organ content of various intestinal enzymes and their localization to assess the relative contribution of intestinal metabolism to overall metabolism.

The distribution of P-450 enzymes is relatively homogeneous in the liver (Debri *et al.*, 1995). However, the distribution of these enzymes is not uniform along the length of the small intestine nor along the villi within a cross-section of mucosa. Longitudinal distribution of total cytochrome P-450 and its functional activity have been measured by CO-binding spectra and aldrin epoxide activity in human small intestinal mucosa. Both the content and activity of cytochrome P-450 was higher in the proximal than that in the distal small intestine (Peters and Kremers, 1989). The average total cytochrome P-450 content in human intestine, about 20 pmol/mg microsomal protein, was found to be much lower than that in the liver (300 pmol/mg microsomal protein) (Peters and Kremers, 1989; Shimada *et al.*, 1994). Immunoblotting studies have shown that CYP3A4 was the dominant cytochrome P-450 in the human small intestine where it accounted for the majority of total microsomal P-450 found in the mucosal epithelium (Watkins *et al.*, 1987; McKinnon *et al.*, 1995). In a recent study, it has been shown that CYP3A4 expression varies along the length of the small intestine. Median values of 31, 23, and 17 pmol/mg microsomal protein were measured in human duodenum, distal jejunum, and distal ileum, respectively (Thummel *et al.*, 1997). The localization and distribution of

CYP3A4 along the villi in human small intestine also has been studied by immunoreactivity using a monoclonal antibody to this major form of human hepatic cytochrome P-450. The columnar absorptive epithelial cells of the villi exhibited the strongest immunoreactivity, whereas no immunostaining was detectable in the goblet cells or the epithelial cells in the crypts (Murray *et al.*, 1988).

A similar differential distribution of intestinal P-450 was observed in animals. P-450 content also varied along the villus in rats, where the P-450 content at the villus tip was approximately 10-fold higher than that at the crypts (Hoensch *et al.*, 1976). Furthermore, CYP1A1 has been detected by immunochemical localization in rat duodenum, but was below detectable levels in the jejunum and ileum. CYP2B1/2 and CYP3A1/2, however, were detected in all three regions, again with the highest levels in the duodenum (de Waziers *et al.*, 1990).

The comparative hepatic and intestinal distribution of cytochrome P-450 in humans has been investigated in detail by de Waziers *et al.* (1990) using immunoblotting techniques. CYP3A4 was found to be the most abundant P-450 in both human liver and small intestine, although the liver exhibited a 2- to 5-fold higher level of the enzyme than the intestine. The levels of CYP3A4 were estimated to be 350 pmol/mg microsomal protein in the liver and 160, 120, and 70 pmol/mg microsomal protein in the duodenum, jejunum, and ileum, respectively (de Waziers *et al.*, 1990). In another study, Watkins *et al.* (1987) showed that the level of CYP3A4 in the human jejunum was comparable to that in the liver, approximately 70 pmol/mg microsomal protein. Although the concentration of CYP3A4 protein in human intestine is comparable to, or somewhat lower than, that determined in the liver, the

estimated total mass of CYP3A4 in the whole intestine was roughly 30 times lower than that in the whole liver (de Waziers *et al.*, 1990). A similar factor (20 times) was reported by Back and Rogers (1987). This difference in total mass of CYP3A4 is related to the very low yield of microsomal protein for the small intestine as compared with the liver because of the localization of the intestinal cytochrome P-450 mainly in villous tip cells, which account for only a very small fraction of the total intestinal cell population (Pacifici *et al.*, 1988). Furthermore, the human liver (*ca.* 1.5 kg) by weight is about twice as large as the small intestine (*ca.* 0.7 kg). Other isoforms detected in human intestine are CYP2C and CYP2D6, whereas CYP1A2 and CYP2E1 were not detected (de Waziers *et al.*, 1990). The estimated total mass of CYP2C and CYP2D6 in the whole intestine was 100 to 200 times lower than that in the whole liver (de Waziers *et al.*, 1990).

Depending upon the segment of small intestine used and the method used for enterocyte isolation, a varying population of epithelial cells will be obtained. Indiscriminate scraping of enterocytes from the intestinal mucosa of the small intestine yields a mixture of villus tip, midvillus, and crypt cells which, when combined, exhibit a low content of P-450. This is due to the absence of the enzyme in the crypt and goblet cells. The uneven distribution of enzymes and isolation of enterocytes complicate *in vitro* studies on intestinal metabolism and probably represent the basis for frequent contradictions in published reports. For example, the mean CYP3A4 content (120 pmol/mg microsomal protein) in human jejunum reported by de Waziers *et al.* (1990) is much greater than the value (70 pmol/mg microsomal protein) cited by Watkins *et al.* (1987) and the value (23 pmol/mg

microsomal protein) reported by Thummel *et al.* (1997). It should be noted that there are significant interindividual differences in level of CYP3A4 expression in intestine. The interindividual differences may also contribute to the discrepancy in the intestinal CYP3A4 level reported by different laboratories. Thus, caution should be exercised when comparisons are being drawn between data from different laboratories.

As seen in humans, the levels of P-450 isoforms also are much lower in the rat small intestine than in the rat liver. Although CYP2C11, the major P-450 isoform in male rats, was present at a high concentration in liver (640 pmol/mg microsomal protein), this isoform was not detectable in the small intestine (de Waziers *et al.*, 1990). Rat CYP1A2 and CYP2E1 also were detectable in the liver, but again not in the small intestine. On the other hand, the concentrations of CYP2B1/2 were comparable in both the liver and the intestine, approximately 90 pmol/mg microsomal protein (de Waziers *et al.*, 1990). Taking the yield of microsomal protein into consideration, in terms of total mass, total amounts of CYP2B1/2 in the whole small intestine was about 30 times lower than those in the whole liver (de Waziers *et al.*, 1990).

Consistent with the P-450 enzyme protein levels, enzymes activity of P-450 isoforms are also higher in the liver than the small intestine. In a study with human hepatic and intestinal microsomes, the CYP3A4 catalytic activities, as measured by erythromycin demethylation, were estimated to be 2.8, 1.6, 1.1 and 0.15 nmol/min/mg microsomal protein in the liver, duodenum, jejunum, and ileum, respectively (de Waziers *et al.*, 1990). Midazolam, a commonly used short-acting benzodiazepine, is metabolized exclusively by CYP3A4 and gives rise to a single major metabolite, 1'-

hydroxymidazolam, which is formed by both human hepatic and intestinal microsomes. The metabolic clearance (V_{max}/K_m) was higher in the liver preparations (540 μL/min/mg microsomal protein) than in the small intestine (135 μL/min/mg microsomal protein) (Thummel *et al.*, 1995). Similarly, tacrolimus, an immunosuppressant, is metabolized by CYP3A4 in human liver and small intestine, where the rate of biotransformation was found to be higher in liver (96 pmol/min/mg microsomal protein) than in the small intestine (54 pmol/min/mg microsomal protein) (Lampen *et al.*, 1995). The metabolism of (+)-bufuralol, a substrate of CYP2D6, was studied in human hepatic and intestinal microsomes (Prudksaritanont *et al.*, 1995). Although the K_m values (5-10 μM) were similar in both hepatic and intestinal microsomes, the V_{max} values were much higher in human hepatic microsomes (383 pmol/min/mg microsomal protein) than in intestinal microsomes (3-9 pmol/min/mg microsomal protein). Similar results were observed in rhesus monkeys (Prueksaritanont *et al.*, 1995). The K_m values (7-9 μM) for (+)-bufuralol were similar in monkey hepatic and intestinal microsomes, whereas the liver had a much higher V_{max} than the small intestine (860 versus 3 pmol/min/mg microsomal protein). In rats, the rate of 7-ethoxycoumarin O-deethylation was 20-fold lower in intestinal microsomes compared to that of hepatic microsomes (Shirley *et al.*, 1979). The K_m and V_{max} values for 7-ethoxycoumarin were 62 μM and 123 pmol/min/mg microsomal protein for rat intestinal microsomes, and the respective values for hepatic microsomes were 19 μM and 800 pmol/min/mg microsomal protein.

From these data, it is clear that both the total enzyme-to protein and catalytic activities of P-450 isozymes in the whole small intestine are much lower (20- to 300-fold less) than those in the whole liver, when the yield of microsomal protein is taken into consideration.

1.4 Enzyme kinetics

The general equation for an enzyme-substrate interaction is as follows:

$$E + S \underset{k_{-1}}{\overset{k_1}{\rightleftharpoons}} ES \xrightarrow{k_{cat}} E + P$$

Where S and P are substrate and product concentrations, and E and ES represent unoccupied and complexed enzyme concentrations, respectively. In addition, k_1 and k_{-1} are, respectively, the kinetic constants for substrate-enzyme affinity and dissociation of the ES complex, while k_{cat} is the rate constant for product formation.

For simple enzymatic reactions, the rate of product formation (v) for a single enzyme can be described by the Michaelis-Menten equation (Segel, 1975):

$$v = \frac{V_{max}[S]}{K_m + [S]}$$

where V_{max} is the maximum product formation rate and K_m is the Michaelis-Menten constant.

Metabolism by an organ, such as the small intestine or the liver, can be expressed as intrinsic clearance (CL_{int}) according to Michaelis-Menten kinetics. The CL_{int} is a measure of the summed Michaelis-Menten equation for each individual enzymatic pathway (Wilkinson, 1987).

$$CL_{int} = \sum_{i=1}^{n} \frac{V_{max\,i}}{K_{mi} + [S]}$$

1.5 Intestinal organ clearance

When a single eliminating organ is considered, the rate of drug elimination from that organ is determined not only by its intrinsic clearance, but also by the rate of drug delivery to the organ. Mathematically, the rate of organ elimination is equal to the difference between the rate of drug delivery to the organ in the inflow and the rate of its exit in the outflow. Accordingly, organ clearance (CL_{organ}) is equal to the product of blood flow to the organ (Q) and the arteriovenous concentration difference (C_{in} - C_{out}) normalized to the drug concentration (C_{in}) in the inflow, as defined by the following equation (Wilkinson, 1987):

$$CL_{organ} = \frac{Q(C_{in} - C_{out})}{C_{in}} = Q \cdot E$$

where E, the extraction ratio, is defined as the fraction of the drug entering the organ that is metabolized during its transit through the organ. Therefore, only a portion (1 -

E) of the dose passed through the organ will escape metabolism. During drug absorption, the extraction ratio (E) also is termed "first-pass" or "presystemic" elimination.

Several kinetic models of hepatic clearance that relate intrinsic enzymatic activity and hepatic blood flow have been proposed (Wilkinson, 1987). Despite some differences in describing the elimination characteristics of the liver, in all models the hepatic clearance (CL_H) is determined by the hepatic intrinsic clearance ($Cl_{int,h}$), the unbound fraction of drug in the blood (f_B), and the liver blood flow (Q_h). Among the various models, the well-stirred model probably is the most widely used because of its simplicity. In the well-stirred model, the liver is considered to be a single, well-mixed compartment with intimate mixing between portal and hepatic arterial blood in the sinusoids. It is considered that only unbound drug can diffuse across hepatocytes. Furthermore, the unbound drug in the blood is assumed to be in equilibrium with that in the hepatocytes. Accordingly, the hepatic clearance (CL_H) and hepatic extraction ratio (E_H) for the well-stirred model can be expressed in terms of equations 1 and 2, respectively (Wilkinson, 1987).

$$CL_H = \frac{Q_h \bullet f_B \bullet CL_{int,h}}{Q_h + f_B \bullet CL_{int,h}} \qquad (1)$$

$$E_H = \frac{f_B \bullet CL_{int,h}}{Q_h + f_B \bullet CL_{int,h}} \qquad (2)$$

In principle, the well-stirred model also can be applied to the small intestine, when this eliminating organ is considered as a single homogenous compartment. In fact, the well-stirred model has been adopted for studies on intestinal metabolism by many investigators (Gillette and Pang, 1977; Colburn, 1979; Klippert *et al.*, 1982; Ilett *et al.*, 1990; Thummel *et al.*, 1997; Chiba *et al.*, 1997), despite the anatomical and biochemical differences between the intestine and liver. The intestinal clearance (CL_G) and intestinal extraction ratio (E_G) for the well-stirred model can be expressed in terms of equations 3 and 4, respectively (Wilkinson, 1987).

$$CL_G = \frac{Q_g \bullet f_B \bullet CL_{int,g}}{Q_g + f_B \bullet CL_{int,g}} \tag{3}$$

$$E_G = \frac{f_B \bullet CL_{int,g}}{Q_g + f_B \bullet CL_{int,g}} \tag{4}$$

where Q_g is the mucosal blood flow in the small intestine, and $Cl_{int,g}$ is the intestinal intrinsic clearance. There are several anatomical and biochemical aspects of the small intestine that need special consideration. First, the distribution of drug-metabolizing enzymes is not uniform along the length of the small intestine, nor along the villi from the villous tip to the crypt. Therefore, prediction of drug elimination by the well-stirred model will be less accurate for the small intestine than for the liver, which has a more uniform distribution of enzymes. Another complicating factor to be considered is that the efficiency of intestinal metabolism may vary during the absorptive and postabsorptive phase. During drug absorption, the movement of drug to the site of intestinal metabolism is mediated by simple diffusion from the intestinal

lumen as a result of sequential thermodynamic events. On the other hand, drugs are delivered to the site of intestinal metabolism from the systemic circulation of the mucosal capillaries during the postabsorptive phase and after i.v. administration. Thus, protein binding of drugs in the blood will limit diffusion out of the capillary when drugs are delivered form the systemic circulation, while simultaneously enhancing the "sink" effect of capillary flow by removing drugs form the site of intestinal metabolism during the absorptive phase.

Although the validity of the well-stirred model with respect to intestinal metabolism has not yet been tested carefully, the model appears to predict the intestinal extraction ratio (E_G) reasonably well for low protein-binding drugs, but not for highly protein bound drugs. Using the intestinal intrinsic clearance (V_{max}/K_m) obtained from rat mucosal cells and a literature value for mucosal blood flow, Klippert *et al.* (1982) successfully predicted the intestinal first-pass metabolism of phenacetin, a low protein-binding drug in control and 3-MC-treated rats. Based on *in vitro* data, the intestinal extraction ratio (E_G) was estimated to be in the range of 0.3 to 0.5 for 3-MC-treated rats, a value which was in good agreement with the measured *in vivo* extraction ratio of 0.5. Similarly, Chiba *et al.* (1997) predicted the *in vivo* intestinal extraction ratio (E_G) of indinavir (a low protein-binding drug) reasonably well from *in vitro* data. However, the intestinal well-stirred model did not accurately predict the extraction ratio (E_G) of midazolam, a high protein-binding drug (more than 96% bound to plasma proteins). Thus, using an intestinal intrinsic clearance (V_{max}/K_m) value of 154 ml/min (Paine *et al.*, 1997) and the reported mucosal blood flow of 250 ml/min (Hulten *et al.*, 1977), the intestinal extraction ratio (E_G) for

midazolam in humans was estimated to be only 0.06 when protein binding (f_B = 0.04) was taken into account (Thummel *et al.*, 1997). This *in vitro* E_G was much lower than the *in vivo* E_G (0.43) determined in liver transplant patients during the anhepatic phase (Paine *et al.*, 1996). However, a better estimate of the *in vitro* E_G (0.35) of midazolam was obtained when protein binding was not taken into consideration (Paine *et al.*, 1997). These results led to speculation by Thummel *et al.* (1997) that protein binding is not an important factor in intestinal first-pass metabolism. Whether plasma protein binding influences the vectoral movement of drug from the intestinal lumen and the extent of intestinal first-pass metabolism remains to be examined.

The intestine epithelium is considered to be much less permeable to drugs than are hepatocytes, making permeability more important when dealing with quantitative aspects of intestinal first-pass metabolism. In addition, because the intracellular residence time of a drug during absorption is determined by two competing processes, the rate of drug absorption and the rate of drug removal from the enterocytes by circulation blood flow, Noordhoek and his coworker (Klippert *et al.*, 1983; Borm *et al.*, 1985) have proposed a new concept of intestinal absorption clearance (CL_{abs}) for the intestinal model for the estimation of the intestinal extraction ratio (E_G). Thus eq.4 can be modified as follows:

$$E_G = \frac{f_B \bullet CL_{int,g}}{CL_{abs} + f_B \bullet CL_{int,g}}$$

Although this model is quite attractive, particularly for those drugs where Cl_{abs} is smaller than mucosal blood flow (Q_g), the validity of the model requires more studies.

Using the $CL_{int,\ g}$ and Cl_{abs} obtained from rat isolated mucosal cells and intestinal perfused segments, this model predicted the *in vivo* E_G for hexamethylmelaine reasonably well, but not for pentamethylmelaine (Klippert *et al.*, 1983; Borm *et al.*, 1985).

1.6 Tissue homogenates and subcellular fractions (S9/microsomes)

These are the simplest and probably most widely used preparations for studying metabolic reactions (Lampen *et al.*, 1995). They provide data on pathways of intestinal xenobiotic metabolism and are eminently suited to screening new drug molecules for presystemic metabolism. Under certain circumstances intrinsic clearance may be used to enable extrapolation to the *in vivo* situation.

1.7 High-performance liquid chromatographic method for the separation of testosterone metabolites

The regio- and stereospecific hydroxylation of the steroid nucleus is a sensitive fingerprint for the identification of a specific CYP isoenzyme (Wood *et al.*, 1983, Sonderfan *et al.*, 1987 and Waxman *et al.*, 1988). For example, CYP2A1 (Wood *et al.*, 1983, Sonderfan *et al.*, 1987) metabolizes testosterone mainly to 7α-hydroxytestosterone, whereas CYP2B1 forms 16α and 16β- hydroxytestosterone (fig. 1.2) (Wood *et al.*, 1983). The metabolism of testosterone has thus been used to

probe *in vitro* preparations of liver and intestine for CYP isoenzyme activities (Wortelboer, *et al.*, 1990, Jayyosi *et al.*, 1992 and Reinerink *et al.*, 1991).

1.8 Rationale for choosing the dog as an animal model

There are a few reasons for choosing the dog as an animal model for *in vitro* studies. First, CYP3A has been identified in the dog's intestinal tissue (Prueksaritanont *et al.*, 1996). Second, 6β-hydroxylation of testosterone has been studied in the dog's jejunum (Prueksaritanont *et al.*, 1996). Third, little is known regarding species differences in the intestinal drug-metabolizing enzymes because most studies of intestinal enzymes have been conducted in rat and human intestines. In the pharmaceutical industry, dogs are common nonrodent species used in early toxicology and metabolism studies of compounds intended for human use. Fourth, it is desirable to provide information that will identify the dog as a useful animal model for the study of intestinal drug metabolism.

Figure 1.2 Metabolic pathways of testosterone.

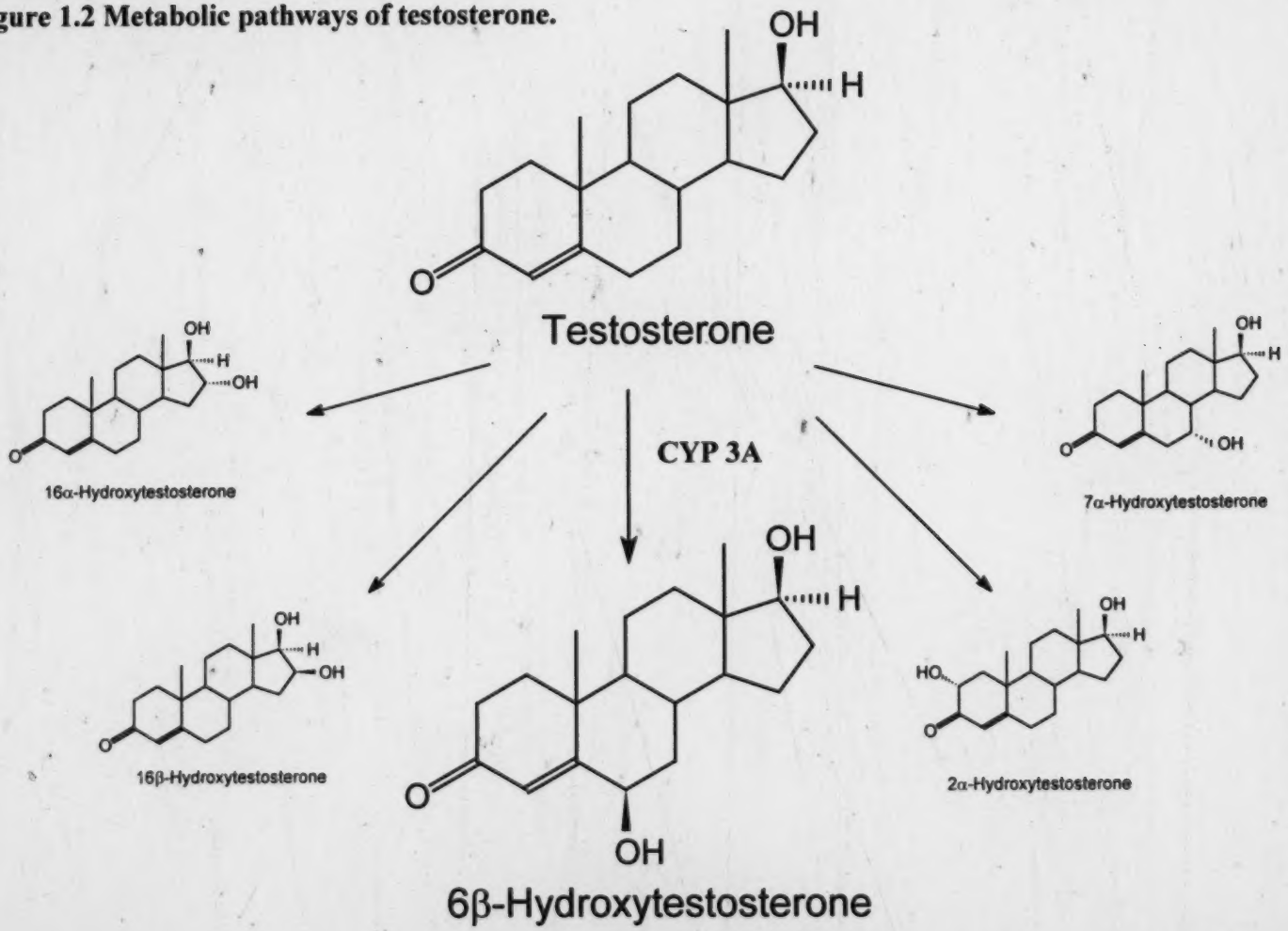

1.9 Hypothesis

The catalytic activity of CYP3A is not uniform along the length of the small intestine in dog.

1.10 Objectives

1. To quantify the catalytic activity of CYP3A in a 1-foot segment from the entire length of four dogs' small intestines.
2. To quantify V_{max}, K_m, and CL_{int} in each intestinal region of four dogs' small intestines.

2. EXPERIMENTAL SECTION

2.1 Materials and chemical reagents

Testosterone powder and testosterone metabolites, 4-androsten-6β, 17β-diol-3-one, 4-androsten-16β, 17β-diol-3-one, 4-androsten-2α, 17β-diol-3-one, 4-androsten-7α, 17β-diol-3-one, and 4-androsten-16α, 17β-diol-3-one and the internal standard, cortexolone, were purchased from Steraloids Inc. (Ottawa, Ontario, Canada). Solvents such as acetonitrile, methanol and methylene chloride (purchased from BDH Inc., Toronto, Ontario, Canada) were HPLC grade.

Potassium chloride and the ingredients of potassium phosphate buffer (purchased from BDH Inc., Toronto, Ontario, Canada) were ACS grade. Glycerol (>99%), a reduced form of NADPH , disodium ethylenediaminetetraacetate (EDTA) and phenylmethylsulfonylfluoride (PMSF) were purchased from Sigma Chemical Co. (St. Louis, MO, USA). Bio-rad reagent was supplied by Bio-Rad Laboratories (Richmond, CA, USA).

2.2 *In vitro* studies using dog intestines

2.2.1 Animals

Surgical and experimental protocols were approved by the Health Sciences and Animal Welfare Committee at the University of Alberta. Random source, healthy female mongrel dogs (total n = 4) were supplied by Biosciences Animal Services, University of Alberta. Dogs were housed in facilities with a controlled temperature

(22 ^{0}C). Diet, composed of Tuffy's chunk (Star Kist Foods, Willowdale, Canada) and Dr. Ballard canned meat (Friskies Pet Care, Don Mills, Canada), was given once daily. Dogs were allowed to have free access to water.

2.2.2 Organ Procurement

Dogs (n = 4) were put on an overnight fast. This is to minimize debris inside the small intestine. Dogs were sacrificed with an i.v. pentobarbital overdose. The small intestines were quickly excised and the lumens were perfused with 4 liters of ice-cold 1.15% KCl with PMSF (0.1 mM). Small intestines were divided into duodenum, jejunum and ileum by the pathologist who euthanized the dog. The small intestines were then transported on ice to a cold room where the intestine was further cut into 1 foot section and weighed. A longitudinal cut was made along the lumen of the small intestine. Mucosal layer was then isolated by scraping using a glass slide, and weighed. Mucosal tissue was stored in 50-mL polypropylene centrifuge tubes at -80 ^{0}C. Mucosal tissue was isolated and frozen within 2 hours of blood flow termination to the organ.

2.2.3 Preparation of intestinal microsomes

Intestinal microsomes were prepared according to the method of Fitzsimmons and Collins (1997) with some modifications. All steps were performed at 4 ^{0}C. Canine mucosal tissue was diluted 1:1 with homogenization buffer (0.154 M KCl, 0.1 M phosphate buffer, 1 mM EDTA; pH 7.4) and homogenized using a glass

homogenizer equipped with a glass pestle (Glas-Col® , Cole-Parmer Instrument Co., Terre Hautein, IN, USA). The homogenate was centrifuged at 12,000g for 20 minutes using a Model IEC B-20A centrifuge equipped with a No. 870 rotor (International Equipment Company, Boston, MASS, USA). The supernatant was decanted and saved. The pellet was suspended with an additional one volume of the same homogenization buffer, the suspension was homogenized and the homogenate was centrifuged at 12,000g for 20 minutes. Supernatants from the 12,000g centrifugations were combined and evenly distributed into polycarbonate tubes (Ultratube®, 13 x 64 mm, Nalge Company, Rochester, NY, USA) and the tubes were centrifuged at 105,000g for 60 minutes in a Model L8-55 ultracentrifuge (Beckman® Instruments Inc., Palo Alto, CA, USA; rotor type 503 Ti). The supernatant was decanted, the pellet was suspended in homogenization buffer, and the homogenate was centrifuged again at 105,000g for 60 minutes. The microsomal pellet was resuspended in homogenization buffer containing 20% v/v glycerol (Sigma Chemical Co., St. Louis, MO, USA) and aliquoted into 0.2 ml fractions and stored at -80 ^{0}C.

2.2.4 Determination of microsomal protein content

Microsomal protein was quantified using the Bradford method (Bradford *et al.*, 1976). Standard curve was prepared using bovine serum albumin (Bio-Rad Laboratories, Richmond, CA, USA). Bovine serum albumin powder was reconstituted with an appropriate volume of water to give a stock solution of 0.4 mg/ml. Aliquots of the stock solution (0, 2, 4, 6, 8, 10, 12 μL) were added in

triplicates to the wells of a microtiter plate (Cell Wells™ 96 well plate, Corning Laboratory Sciences Co., Richmond Hill, Ontario, Canada). Sufficient volumes of the Bio-rad reagent were added such that the final volume in each well was 200 μL. For the determination of protein concentration of intestinal microsomes, the original sample was diluted by a factor of 1/25 to 1/500. Triplicate aliquots (10 μL) of each diluted samples were each mixed with 190 μL of the Bio-rad reagent. Absorbance readings were taken at 590 nm using a Molecular Devices MAXline microtitre plate reader.

2.2.5 Incubation studies

A microsomal reaction mixture (final volume, 1 ml) containing microsomal protein (1 mg/ml), 5 mM $MgCl_2$, 5 μM $MnCl_2$, 1 mM NADPH in 100 mM potassium phosphate buffer (pH 7.4) was pre-incubated at 37 ^{0}C for 5 minutes. The reaction was initiated by adding aliquots (10 μL) of various testosterone stock solutions to the mixture and carried out in air in microcentrifuge tubes (Brinkmann Instruments Inc., Westbury, NY, USA) at 37 ^{0}C. Substrate concentrations in incubation mixtures ranging from 25 μM to 500 μM were studied. Incubation time was 10 minutes. The reaction was terminated by the addition of 6 ml of dichloromethane.

To evaluate inter-day variability in incubation procedures, same batch of intestinal microsome was incubated with testosterone at different concentration in duplicates on eight separate occasions.

2.2.6 Instrumentation and chromatographic conditions

The HPLC system (HP Series 1100) was equipped with a diode array UV detector set at 247 nm and an IBM-compatible PC computer equipped with HP ChemStation software program. Chromatographic resolution of testosterone and its metabolites was achieved using an Agilent Eclipse® XDB-C8 column (3.5 μm, 4.6 x 75 mm, Agilent, Wilmington, DE, USA).

An isocratic elution method was used for the quantification of 4-androsten-6β, 17β-diol-3-one in intestinal microsome samples. The mobile phase composition was a mixture of distilled, deionized water and acetonitrile (73:27 v/v). Flow rate was 1.0 mL/min. Temperature was at 45 ^{0}C. The total run time was 21 min.

2.2.7 Standard solution

Standard stock solution of testosterone and 4-androsten-6β, 17β-diol-3-one were prepared in methanol and stored at -20 ^{0}C. Serial dilution with the microsomal mixture was then made to give various concentrations for the calibration curves.

Calibration curves were linear over a range of 0.1 μM - 20 μM for 4-androsten-6β, 17β-diol-3-one ($r>0.998$). Assay procedures were validated by comparing results with quality control samples prepared by other colleagues in the laboratory. Duplicates of two different concentrations were prepared and analyzed together with

standard and unknown samples. The intra- and inter-day coefficients of variation for accuracy and precision of all analytes were <15%.

2.2.8 Sample preparation

1 mL of incubation mixture was transferred from a microcentrifuge tube (Brinkmann Instruments Inc., Westbury, NY, USA) to a glass tube (16 mm x 100 mm, Kimax®, Kimble, IL, USA), to which 70 µL of cortexolone (14.4 µM) was added as internal standard. Each sample was extracted with 6 mL of dichloromethane by shaking for 10 min using a vortex shaker (IKA-VIBRAX-VXR, Terochem Laboratories Ltd., USA) and centrifuged at 1,800 x g (Dynac centrifuge, Clay Adams, USA) for 10 min. The organic layer was transferred into clean glass tubes (13 x 100 mm, Kimax®, Kimble, IL, USA) and was then dried using the Savant Speedvac centrifugal vacuum evaporation system (Model SC 100, Savant Instruments Inc., Farmingdale, NY, USA). The residues were reconstituted with 40 µL of methanol and 90 µL of water. 50 µL of the solution was injected into the HPLC system.

2.2.9 Enzyme kinetics analysis

Enzyme kinetic parameters were determined by linear regression of transformed data using EnzymeKinetics (Stanislawski, 1993). The data were fitted using the Michaelis-Menten equation as follows,

$$v = (V_{max}\,[s])/(K_m + [s])$$

2.2.10 Statistical analysis

ANOVA was used to detect differences in all kinetic parameters among the duodenum, jejunum and ileum samples. All tests were conducted at the 0.05 level of significance. Values are reported as mean ± SD.

3. RESULTS

3.1 Method development

A representative chromatogram showing the separation of testosterone, its five metabolites and internal standard (cortexolone) is shown in Figure 3.1. A representative chromatogram from a sample containing testosterone after incubation with dog intestine microsomes is shown in Figure 3.2. The retention times of testosterone, cortexolone, and 6β-hydroxytestosterone were approximately 19.0, 10.0 and 3.0 min, respectively. A calibration curve for 6β-hydroxytestosterone is shown in Figure 3.3. Excellent correlation was observed for this compound. The UV spectrum (190 nm - 300 nm) of 6β-hydroxytestosterone in a dog intestine microsome sample is superimposable on that of authentic 6β-hydroxytestosterone (Figure 3.4) which demonstrates the purity of the metabolite peak.

3.2 Precision and accuracy of HPLC method

Inter-day precision and accuracy of the method were determined from back-calculated results for the five calibration standards for 6β-hydroxytestosterone from three runs. Intra-day precision was determined by assaying three replicates at each of five different concentrations of 6β-hydroxytestosterone in one analytical run. The results are shown in Table 3.1. Intra-day and inter-day precision (expressed as

coefficient of variation) was less than 15% for all concentrations of 6β-hydroxytestosterone. Accuracies ranged from 91.1% to 117.5% for 6β-hydroxytestosterone.

3.3 Extraction recovery

The extraction recovery of the analytes was determined by comparing the peak areas of spiked microsomal samples extracted with methylene chloride to the peak areas of standard solutions at the same concentration not carried through the extraction procedure. Mean percentage recoveries for 6β-hydroxytestosterone was 94% ± 2% (n = 3).

3.4 Inter-day precision of determination of enzymatic activities

Except for one sample, overall inter-day precision were within 12% (Table 3.2). The effect of substrate concentration on testosterone metabolism is illustrated in Figure 3.5.

3.5 Distribution of intestinal CYP3A activities

For three out of four intestines (#1, #2, #3), CYP3A catalytic activity decreased from duodenum to middle jejunum and then increased in middle jejunum and

declined thereafter to ileum (figure 3.6, 3.7, 3.8, 3.9). For #4, CYP3A catalytic activity went up and down throughout the small intestine without a specific pattern. CYP3A catalytic activity between sections of an intestine ranged from 3-fold to 10-fold.

3.6 Testosterone 6β- hydroxylation kinetics

Four intestines were examined for regional (duodenal, jejunal, and ileal) testosterone 6β- hydroxylation kinetics. Eadie-Hofstee plots of 4-anderosten-6β 17β-diol-3-one formation kinetics for one of the three intestinal regions of four small intestines are shown in figure 3.10. Kinetic parameters for the formation of 4-androsten-6β, 17β-diol-3-one in dog intestinal microsomes are shown in Table 3.3. Average (± SD) K_m values were 93 (± 16.12), 102.8 (± 11.5) and 100.3 (± 63.22) μM for duodenum, jejunum and ileum, respectively (Figure 3.11). ANOVA revealed no differences in K_m values among the three tissues (p = 0.72). Average (± SD) V_{max} values were 157 (± 56.31), 89 (± 20.22), 54.3 (± 30.14) pmol/min/mg for duodenum, jejunum and ileum, respectively (Figure 3.12). ANOVA revealed a statistically significant difference in V_{max} between duodenum and ileum (p = 0.0045) and duodenum and jejunum (p = 0.0346), but not between jejunum and ileum (p = 0.2357). Average (± SD) intrinsic clearances ($Cl_{in,mic}$) for duodenum, jejunum and ileum were 1.69 (± 0.52), 0.89 (± 0.28), and 0.61 (± 0.39) μL/min/mg (Figure 3.13). ANOVA revealed a statistically significant difference in $Cl_{in,mic}$ between duodenum

and ileum (p = 0.0045) and duodenum and jejunum (p = 0.0217), but not between jejunum and ileum (p = 0.3480).

Table 3.1 Precision and accuracy of 6β-hydroxytestosterone calibration standards.

Standard amount (pmol)	Mean calculated amount (pmol)	Accuracy (%)	Inter-day (n=3) CV (%)	Intra-day (n=3) CV (%)
62.5	73.45	117.52	14.74	4.29
125	125.68	100.54	11.77	0.96
250	235.87	94.35	12.76	2.19
500	455.50	91.1	7.27	3.15
1000	976.83	97.68	8.15	11.22

Table 3.2 Inter-day precision of determination of enzymatic activities in dog intestine microsomes.

Sample	v (day 1) (pmol/min/ mg)	v (day 2) (pmol/min/ mg)	Average v (pmol/min/ mg)	SD	CV(%)
#1 DA	83.73	70.88	77.30	9.09	11.76
#1 DB	69.59	73.05	71.32	2.45	3.43
#1 DC	54.03	60.36	57.20	4.47	7.82
#1 JD	18.11	17.36	17.74	0.53	2.99
#1 JE	10.17	9.15	9.66	0.72	7.48
#1 IA	23.75	27.16	25.45	2.41	9.48
Jan26 IA	71.61	70.30	70.96	0.93	1.31
#2 J6	190.80	264.00	227.40	51.76	22.76

Table 3.3 Kinetic parameters for the formation of 6β-hydroxytestosterone in dog intestinal microsomes. Simple Michaelis-Menten equation[a]:

	Dog intestinal microsomes: Duodenum			
	#1	#2	#3	#4
V_{max} (pmol/min/mg)	93	224	134	177
K_m (μM)	92	116	84	80
Cl_{int} (μL/min/mg)	1.01	1.93	1.60	2.21
r	0.984	0.996	0.981	0.970

	Dog intestinal microsomes: Jejunum			
	#1	#2	#3	#4
V_{max} (pmol/min/mg)	63	104	83	106
K_m (μM)	117	89	104	101
Cl_{int} (μL/min/mg)	0.54	1.17	0.80	1.05
r	0.998	0.970	0.995	0.976

	Dog intestinal microsomes: Ileum			
	#1	#2	#3	#4
V_{max} (pmol/min/mg)	28	74	29	86
K_m (μM)	68	195	66	72
Cl_{int} (μL/min/mg)	0.41	0.38	0.44	1.19
r	0.996	0.993	0.993	0.976

[a] Nonlinear regression analysis (substrate concentrations range from 25 - 500 μM).

Figure 3.1 Representative chromatogram of blank microsomes spiked with testosterone, its five metabolites and internal standard (IS). (7α: 7α-hydroxytestosterone, 6β: 6β-hydroxytestosterone, 16α: 16α-hydroxytestosterone, 16β: 16β-hydroxytestosterone, 2α: 2α-hydroxytestosterone, IS: Cortexolone).

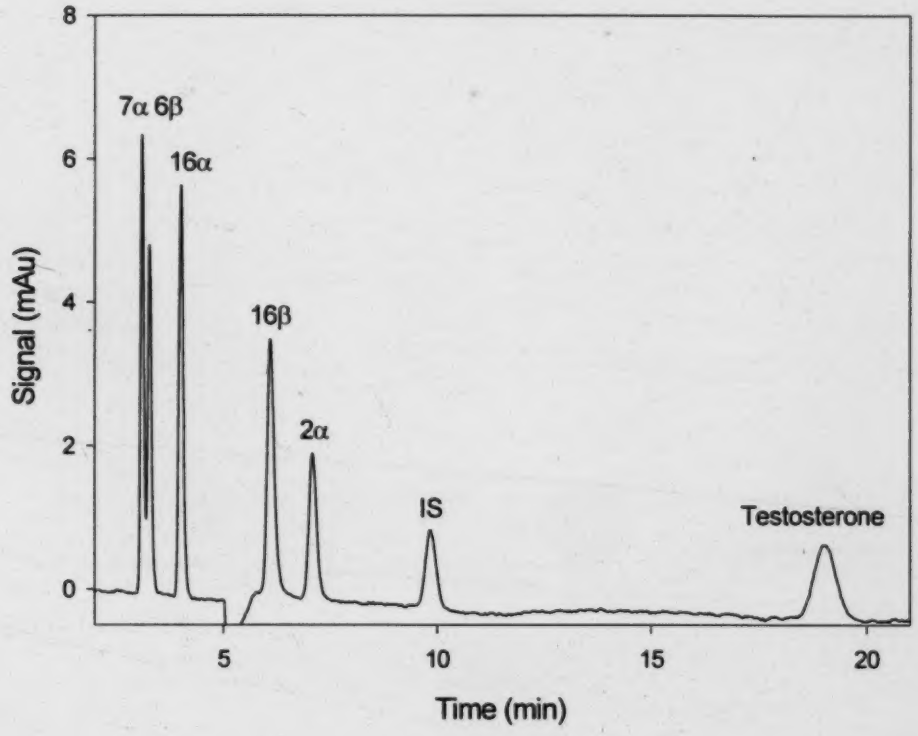

Figure 3.2 A representative chromatogram of a testosterone sample spiked with internal standard after 10 minutes of incubation with dog intestinal microsomes.

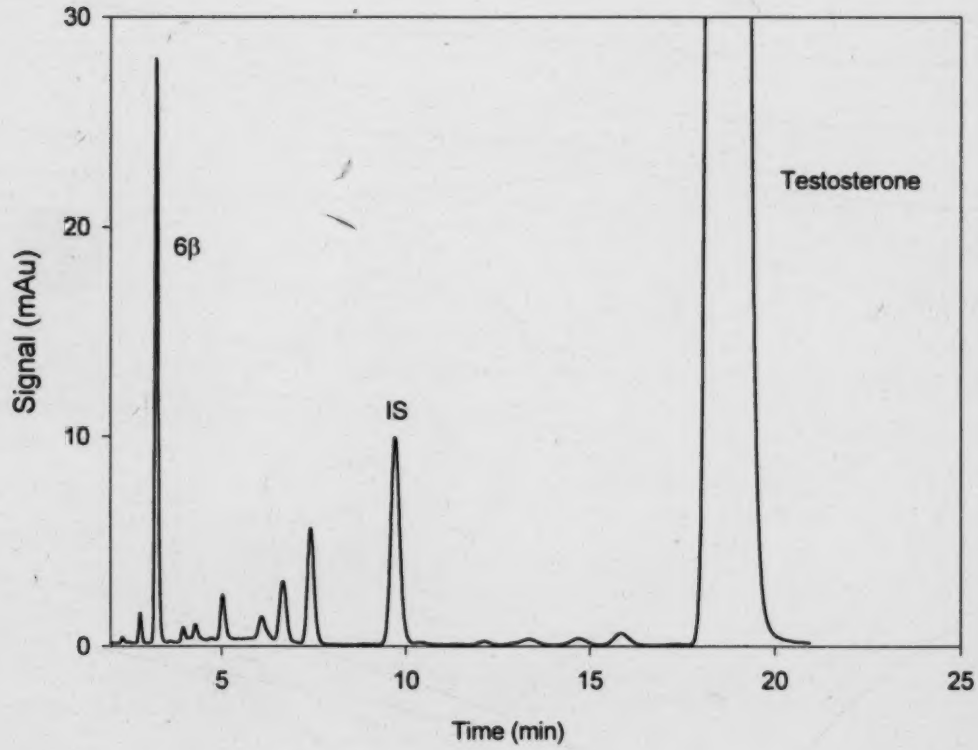

Figure 3.3 Calibration curve for 6β-hydroxytestosterone using the internal standard method.

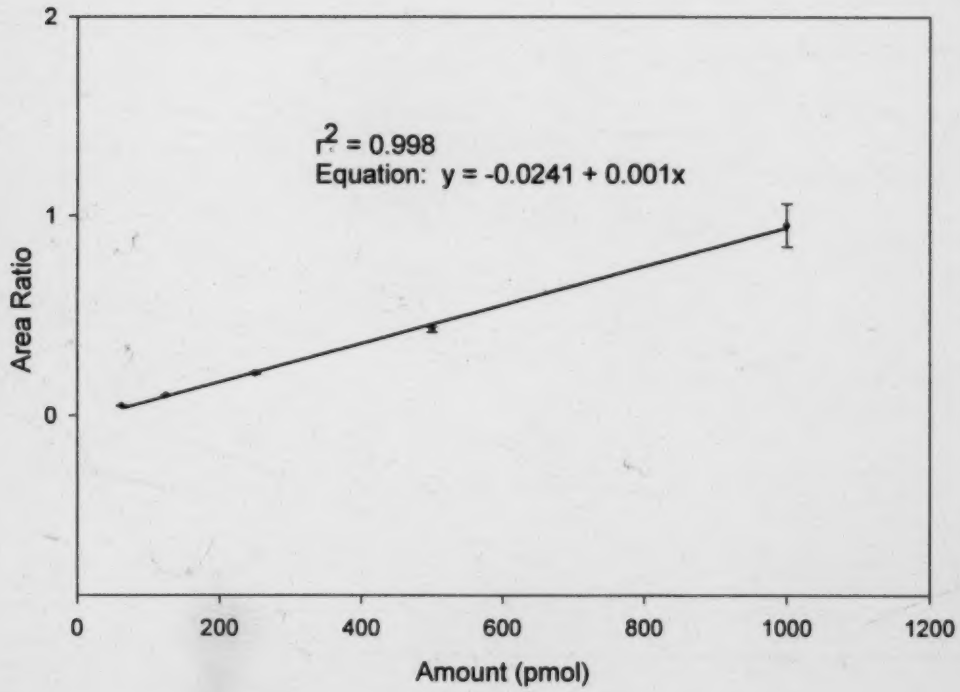

Figure 3.4 A typical diagram showing that the UV spectrum (190 - 300 nm) of the 6β-hydroxytestosterone peak in a dog intestine microsome sample (- - -) is superimposable on that of authentic 6β-hydroxytestosterone (------).

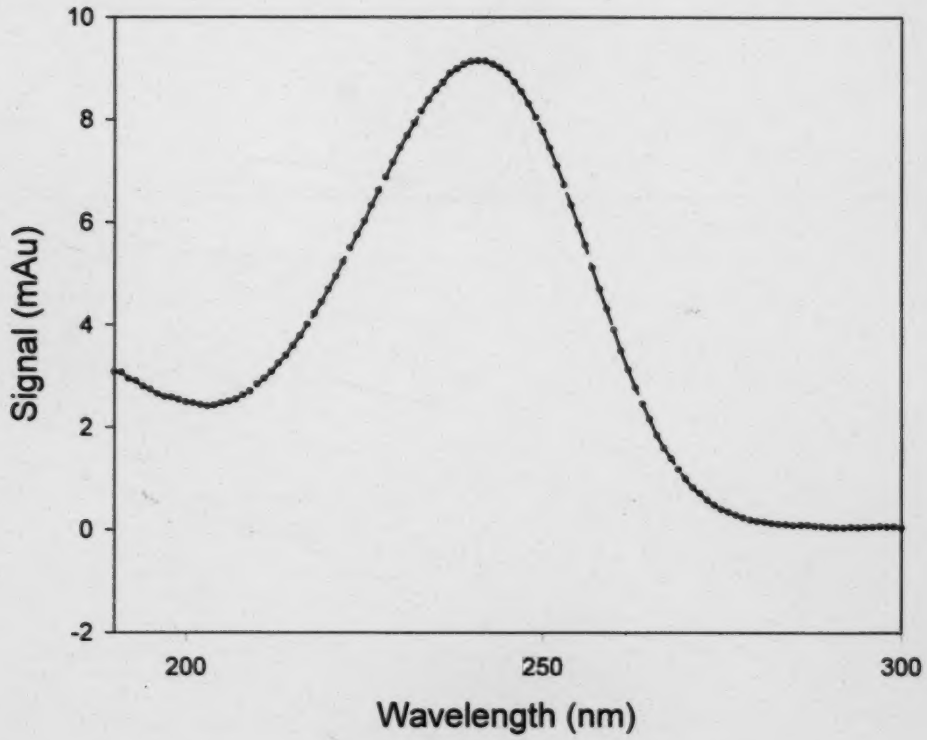

Figure 3.5 Effect of substrate concentration on the rates of 6β-hydroxylation of testosterone.

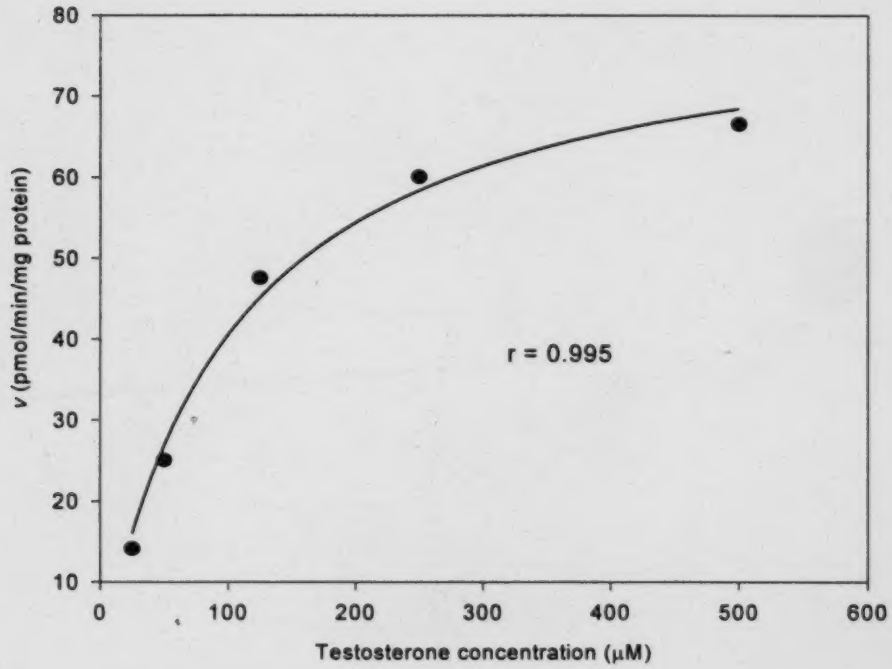

Figure 3.6 Longitudinal testosterone 6β-hydroxylation rates (at 500 mM testosterone) for dog #1's small intestine.

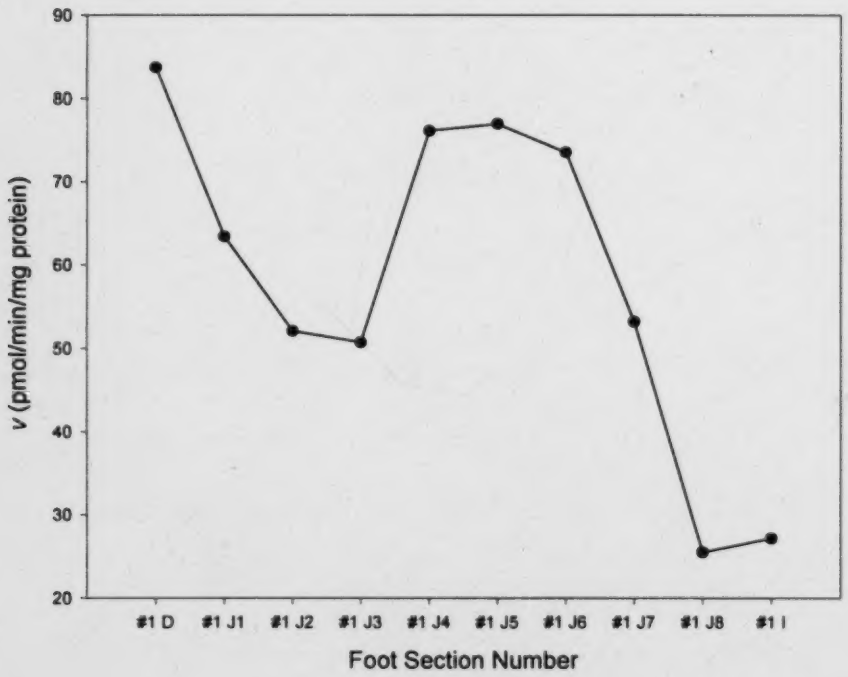

Figure 3.7 Longitudinal testosterone 6β-hydroxylation rates (at 500 mM testosterone) for dog #2's small intestine.

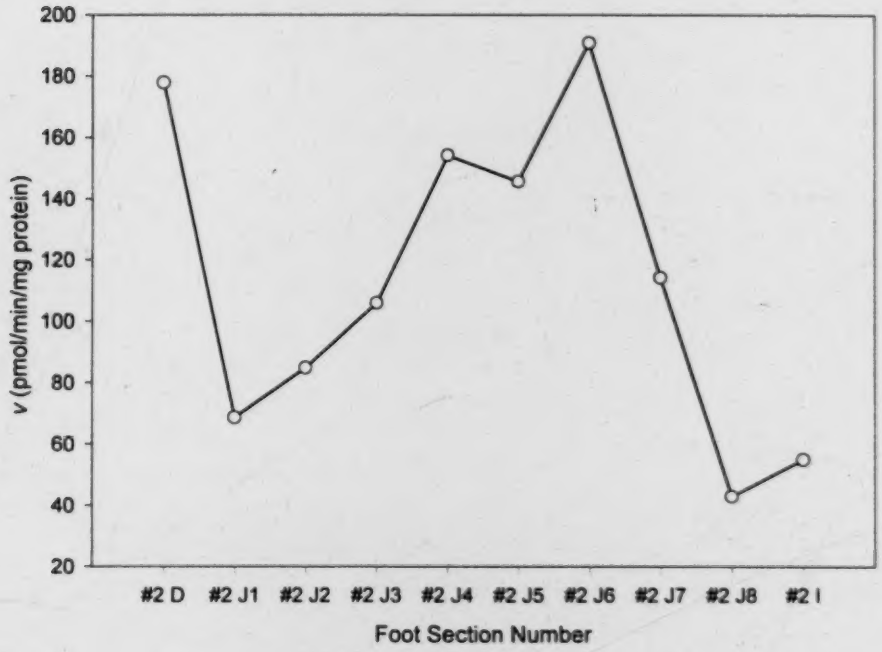

Figure 3.8 Longitudinal testosterone 6β-hydroxylation rates (at 500 mM testosterone) for dog #3's small intestine.

Figure 3.9 Longitudinal testosterone 6β-hydroxylation rates (at 500 mM testosterone) for dog #4's small intestine

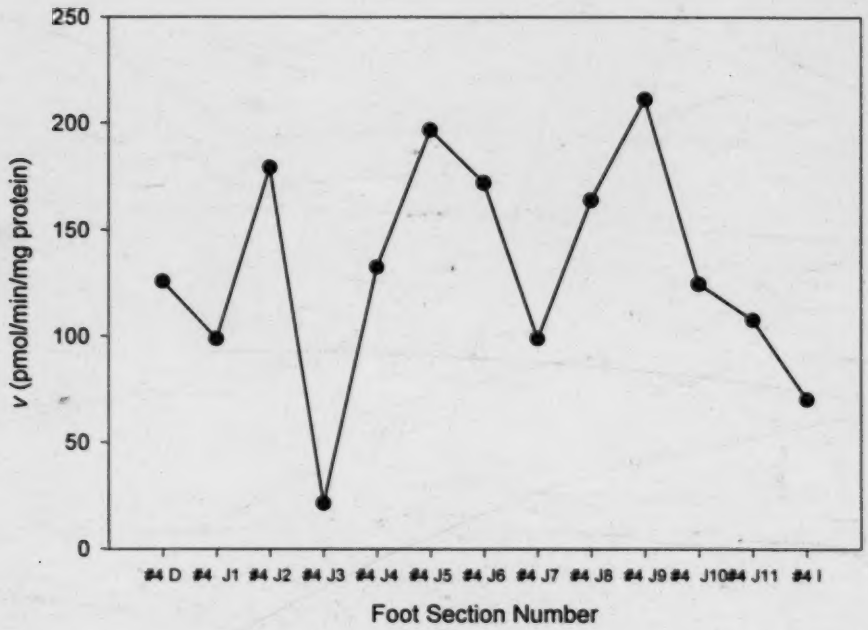

Figure 3.10 Representative Eadie-Hofstee plot of 6β-hydroxytestosterone formation in dog intestine microsomes.

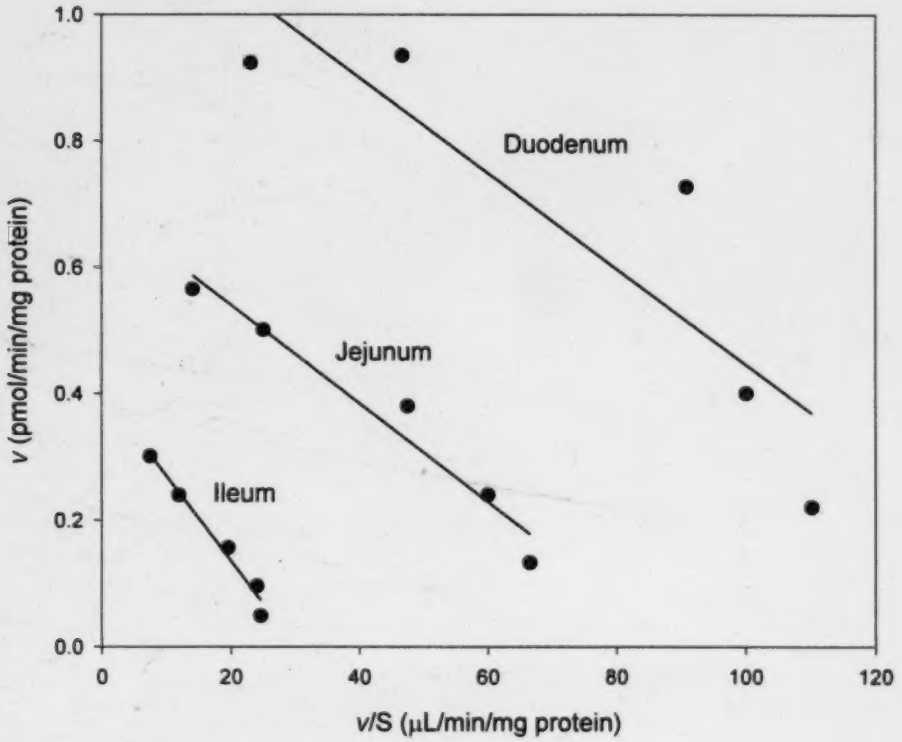

Figure 3.11 Average K_m values for duodenum, jejunum and ileum of four dogs' small intestines. ANOVA revealed no differences in K_m values among the three tissues (p = 0.72).

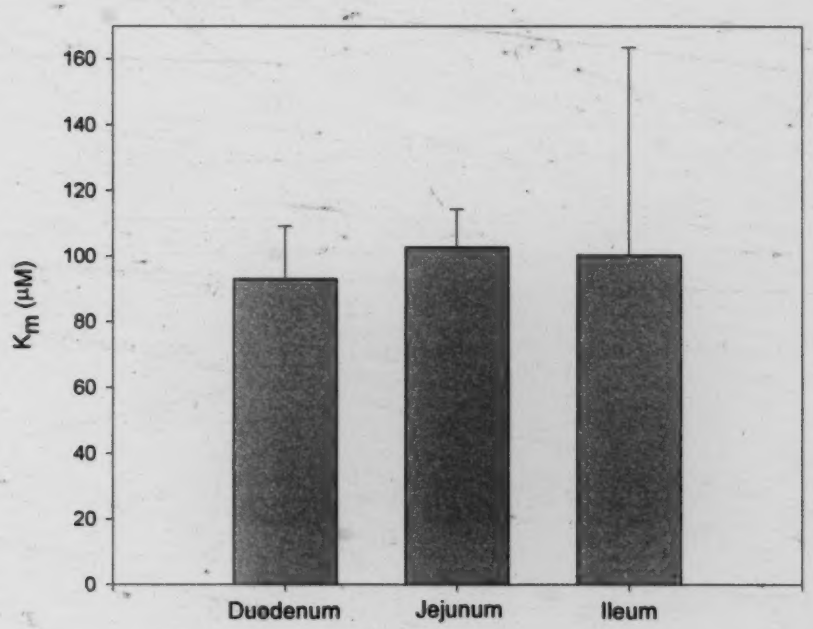

Figure 3.12 Average V_{max} values for duodenum, jejunum and ileum of four dogs' small intestines. ANOVA revealed a statistically significant difference in V_{max} between duodenum and ileum ($p = 0.0045$) and duodenum and jejunum ($p = 0.0346$), but not between jejunum and ileum ($p = 0.2357$).

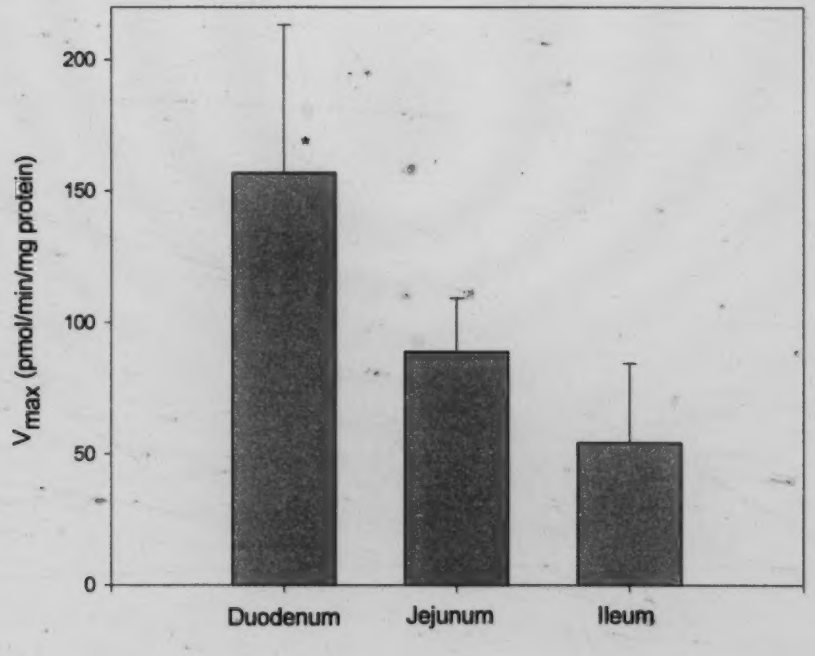

Figure 3.13 Average CL_{int} values for duodenum, jejunum and ileum of four dogs' small intestines. ANOVA revealed a statistically significant difference in $Cl_{int,mic}$ between duodenum and ileum (p = 0.0045) and duodenum and jejunum (p = 0.0217), but not between jejunum and ileum (p = 0.3480).

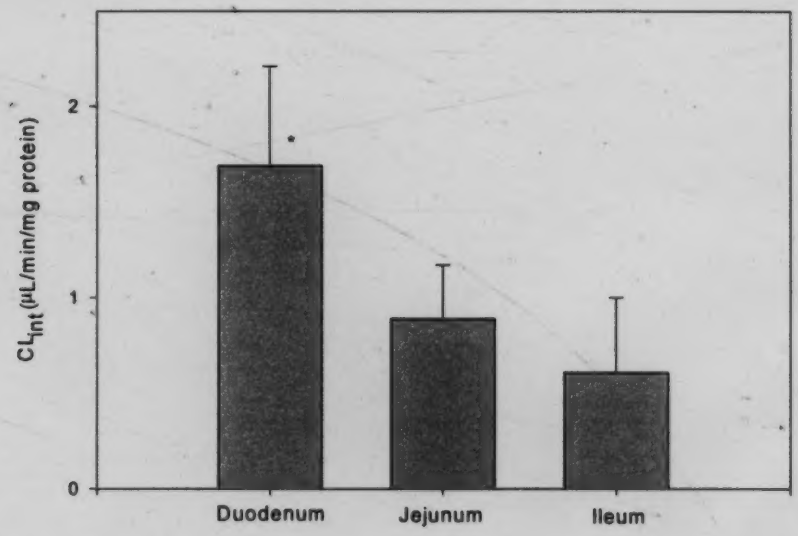

4. DISCUSSION

4.1 Distribution of intestinal CYP3A activities.

Results from this study provide the first characterization of intraintestinal variability in CYP3A metabolic function in dogs. Four full-length intestines were examined of mongrel dogs that were one to five years of age. All the dogs were about 15 to 16 kg, except dog #4 which was 30 kg. All the dogs were healthy with no abnormalities. The organs were also procured under carefully controlled conditions. It was found that for three of four intestines (Dog #1, #2 and #3), CYP3A catalytic activity decreased from duodenum to middle jejunum and then increased in middle jejunum and decreased thereafter in ileum. This is somewhat different from the human findings reported by Paine *et al.* (1997). They found that for four of six human intestines, CYP3A catalytic activity increased from duodenum to middle jejunum and then decreased to distal ileum. They also found that the interindividual variability in CYP3A activities was great which is consistent with results published by Zhang *et al.* (1999). These investigators reported that maximal erythromycin N-demethylase activity varied between 0.30 and 0.76 nmol/min/mg microsomal protein for the 10 human intestines that they studied. This represents a 153% difference among different individuals. In the present study, the maximal testosterone 6β-hydroxylation rate varied between 84 and 211 nmol/min/mg microsomal protein for the 4 dogs in the study. This represents a 151% difference, which is very similar to

the human data. *CYP3A* activities between sections of intestine ranged from 3-fold to 25-fold in humans. In contrast, I found that CYP3A activities between sections of intestine in dogs ranged from 3-fold to 10-fold. Based on my results, intraintestinal variability in CYP3A activities in dogs was less than humans. Since the sample size is small (n = 4) in the present study, a future studies with a larger sample size may be needed to confirm my findings.

4.2 Testosterone 6β-hydroxylation kinetics

I only detected testosterone 6β-hydroxylation activities in dogs' small intestines. No other metabolites of testosterone were detected with my HPLC assay which indicates that CYP3A is the major form of CYP P-450 isoenzyme that exists in the dog intestine. My findings fully agree with results reported by Prueksaritanont *et al.* (1996) who did not detect any bufuralol 1'-hydroxylase or tolbutamide methylhydroxylation activity in beagle dog's intestine. These metabolites are functional markers for human CYP2D6 and CYP2C8-10. This is also true in human in that the small intestine contained high specific content of CYP3A4, as found by Watkins *et al.* (1987) and Peters and Kremers (1989). Therefore CYP3A appears to be the major CYP isoenzyme that resides in both human and dog's small intestines.

I found average V_{max} values of testosterone 6β-hydroxylation activities to be 157, 89 and 54.3 pmol/min/mg microsomal protein in duodenum, jejunum and ileum,

respectively. Prueksaritanont *et al.* (1996) reported average V_{max} values to be 150 pmol/min/mg microsomal protein in jejunum in beagle dogs. They also found that humans and monkeys generally exhibited higher intestinal enzyme activities than dogs. Average V_{max} value was 1580 pmol/min/mg microsomal protein in human jejunum which is about 17 times higher than in mongrel dogs' jejunum. It is clear from *in vitro* data that the activity of CYP3A in dogs' intestine is much lower than that observed in both the human intestine and dog liver. With the limited drug-metabolizing capacity in the small intestine, the contribution of this organ to the overall metabolism of a drug is less likely to be quantitatively as important as that of the liver.

ANOVA revealed a statistically significant difference in average V_{max} values between duodenum and ileum ($p = 0.0045$) and duodenum and jejunum ($p = 0.0346$), but not between jejunum and ileum ($p = 0.2357$) in the present study. This is not in complete agreement with the results of Paine *et al.* (1997) who reported median V_{max} values among all three intestinal regions in humans are statistically significant using ANOVA ($p = 0.0001$). However, Wilcoxon signed-rank tests revealed a significant difference between duodenum and ileum ($p = 0.002$) and jejunum and ileum ($p = 0.005$) but not between duodenum and jejunum ($p = 0.14$) in human (Paine *et al.*, 1996). In the study now reported, the average Cl_{int} was 1.69, 0.89, and 0.61 μL/min/mg microsomal protein in dog's duodenum, jejunum and ileum, respectively. ANOVA revealed a statistically significant difference in $Cl_{in,mic}$ between duodenum

and ileum (p = 0.0045) and duodenum and jejunum (p = 0.0217), but not between jejunum and ileum (p = 0.3480). In contrast, Paine *et al.* (1997) reported median intrinsic clearances for duodenum, jejunum and ileum to be 157, 85, 14 μL/min/mg microsomal protein in humans. ANOVA with subsequent Wilcoxon signed-rank test revealed similar contrasts as those described for V_{max} (Paine *et al.*, 1997).

The CYP3A catalytic activities, as measured by erythromycin demethylation were estimated to be 1.6, 1.1, and 0.15 nmol/min/mg microsomal protein in the duodenum, jejunum and ileum in human, respectively (de Waziers *et al.*, 1990). The ratio of $V_{max\ (duodenum)}$ / $V_{max\ (ileum)}$ is 10.6 in human versus 2.9 in mongrel dogs in my study. The percentage change of regional variability between duodenum and ileum is 91% in human and 65% in mongrel dogs. Therefore, the regional variability among the duodenum, jejunum and ileum seems to be higher in humans than in dogs. However, the general trend of decreasing catalytic activities from duodenum to ileum is common in both species. In contrast, the mRNA expression of p-glycoprotein appeared to increase progressively from the stomach to the colon with low levels in the stomach (5 arbitrary units), intermediate in the jejunum (20 arbitrary units) and high levels in colon (30 arbitrary units) (Fricker *et al.*, 1996). A similar observation was found by other investigators, wherein levels of MDR1 mRNA were measured in normal human tissues (Fojo *et al.*, 1987). The level of mRNA was higher in the colon than in the jejunum by a factor of 2. These results suggest that the expression of p-glycoprotein, contrary to that of cytochrome P-450, increases progressively along the

length of intestine. This reciprocal protein concentration gradient of P-450 and p-glycoprotein expression reflects the perfection of Mother Nature in designing defense systems to protect the body against toxic xenobiotics.

In the present study, average K_m values were found to be 93, 102.8 and 100.3 μM in dog's duodenum, jejunum and ileum, respectively. Prueksaritanont *et al.* (1996) reported a lower K_m value of 60 μM in beagle dogs' jejunum. They also reported a K_m value of 90 μM in human jejunum which is very similar to the K_m value that I found in mongrel dogs' small intestines. I found no statistically significant difference among the three regions of the small intestines which suggests that gut CYP3A levels in all three regions of small intestines are functionally equivalent in dogs. This is in agreement with human data where Paine *et al.* (1997) did not find any statistically significant difference among the K_m values of duodenum, jejunum and ileum ($P = 0.15$).

5. Conclusions

Extensive characterization of intestinal CYP3A metabolic capacity has revealed that the CYP3A catalytic activities are not uniform along the length of a dog's small intestine. For three of four intestines, CYP3A catalytic activity decreased from duodenum to middle jejunum and then increased in middle jejunum and declined thereafter to ileum. There is a 3-fold to 10-fold difference between sections of an intestine. There is a general trend of decreasing CYP3A catalytic activities from duodenum to ileum.

6. References

Back DJ and Rogers SM (1987) First-pass metabolism by gastrointestinal mucosa. Aliment Pharmacol Ther 227: 339-357.

Bertalanffy FD and Nagy KP (1961) Mitotic activity and renewal rate of the epithelial cells of human duodenum. Acta Anat 45: 362-370.

Biber B, Lundgren O and Svanvik J (1973) The influence of blood flow on the rate of absorption of 85 Kr from the small intestine of the cat. Acta Physiol Scand 89: 227-238.

Bond JH, Levitt DG and Levitt MD (1977) Quantitation of countercurrent exchange during passive absorption from the dog small intestine. J Clin Invest 59: 308-310.

Bond JH and Levitt MD (1979) Use of microspheres to measure small intestinal villus blood flow in the dog. Am J Physiol 236: E577-E583.

Bond JH, Prenfiss RA and Levitt MD (1979) The effects of feeding on blood flow to the stomach, small bowel and colon of the conscious dog. J Lab Clin Med 93: 594-599.

Borm PJA, Frankhuyzen-Sierevogel AC, Weller EBC and Noordhoek J (1985) Absorption and metabolism of hexamethylmelamine and pentamethylmelamine in rat everted perfused gut segments: Correction with in-vitro data. J Pharm Pharmacol 37: 629-636.

Caldwell J and Marsh MV (1982) Metabolism of drugs by the gastrointestinal tract, in Clinical Pharmacology and Therapeutics: Presystemic Drug Elimination (George CF, Shand DG andRenwick AG eds) pp 29-42, Butterworths, London.

Campa JL and Reynolds TB (1988) The hepatic circulation, in The Liver Biology and Pathology (Arias IM, Jakoby WB, Popper U, Schachter D and Shafritz DA eds) pp 911-930, Raven Press, New York.

Chen J and Pang KS (1997) Effect of flow on first-pass metabolism of drugs: Single pass studies on 4-methylum-belliferone conjugation in the serially perfused rat intestine and liver preparations. J Pharmacol Exp Ther 280: 24-31.

Chiba M, Hensleigh M and Lin JH (1997) Hepatic and intestinal metabolism of indinavir, an HIV protease inhibitor, in rat and human microsomes. Biochem Pharmacol 53: 1187-1195.

Colburn WA (1979) A pharmacokinetic model to differentiate preabsorptive, gut, epithelial, and hepatic first-pass metabolism: J Pharmacokinet Biopharm 7:407-415.

Creamer B (1967) The turnover of the epithelium of the small intestine. Br Med Bull 23: 226-230.

de Vries MH, Hofman GA, Koster ASJ and Noordhoek J (1989) Systemic intestinal metabolism of 1-naphthol. A study in the isolated vascularly perfused rat small intestine. Drug Metab Dispos 17: 573-578.

Debri K, Boobis AR, Davies DS and Edwards RJ (1995) Distribution and induction of CYP3A1 and CYP3A2 in rat liver and extrahepatic tissues. Biochem Pharmacol 50: 2047-2056.

de Waziers I, Cugenec PH, Yang CS, Lerous JP and Beaune PH (1990) Cytochrome P450 isoenzymes, epoxide hydrolase and glutathione transferase in rat and human hepatic and extrahepatic tissues. J Pharmacol Exp Ther 253:387-394.

Eichelbaum M, Albrecht M, Kliems G, Schäfer K and Somogyi A (1980) Influence of meso-caval shunt surgery on verapamil kinetics, bioavailability and response. Br J Clin Pharmacol 10: 527-530.

Floren LC, Bekersky I, Benet LZ, Mekki Q, Dressler D, Lee JH, Roberts JP and Hebert MR (1997) Tacrolimus oral bioavailability doubles with coadministration with ketoconazole. Clin Pharmacol Ther 62: 41-49.

Fojo AT, Ueda K, Slamon DJ, Poplack DG, Gottesman MM and Pastan I (1987) Expression of a multidrug resistance gene in human tumors and tissues. Proc Natl Acad Sci USA 84: 265-269.

Fricker G, Drewe J, Huwyler J, Gutmann H and Beglinger C (1996) Relevance of p-glycoprotein for the enteral absorption of cyclosporin A: In vitro-in vivo correlation. Br J Pharmacol 118: 1841-1847.

Fromm MF, Busse D, Kroemer HK and Eichelbaum M (1996) Differential induction of prehepatic and hepatic metabolism of verapamil by rifampin. Hepatology 24: 796-801.

Ged C, Rouillon JM, Pichard L, Combalbert J, Bressot N, Bories P, Michel H., Beaune P. and Maurel P (1989) The increase in urinary excretion of 6-hydroxycortisol as a marker of human hepatic cytochrome P450IIIA induction. Br J Clin Pharmacol 28: 373-387.

Gillette JR and Pang KS (1977) Theoretic aspects of pharmacokinetic drug interaction. Clin Pharmacol Ther 22: 627-638.

Gore RW and Bohlen HG (1977) Microvascular pressures in rat intestinal muscle and mucosal villi. Am J Physiol 233:H685-H693.

Guengerich FP (1995) Cytochrome P450 enzymes, in Cytochrome P450: Structure, Mechanism and Biochemistry (Ortiz de Montellano PR ed) pp 473-535, Plenum Press, New York.

Guyton AC (1991) General principles of gastrointestinal function mortality, nervous control, and blood circulation, in Textbook of Medical Physiology pp 698-708, WB Saunders, Philadelphia.

Hallback DA, Hulten L, Jodal M, Lindhagen J and Lundgren D (1978) Evidence for the existence of a countercurrent exchanger in the small intestine in man. Gastroenterology 74: 683-690.

Hebert MF, Roberts JP, Prueksaritanont T and Benet LZ (1992) Bioavailability of cyclosporine with concomitant rifampin administration is markedly less than predicted by hepatic enzyme induction. Clin Pharmacol Ther 52: 453-457.

Hirayama H and Pang KS (1990) First-pass metabolism of gentisamide: Influence of intestinal metabolism on hepatic formation of conjugates: Studies in the once-through vascularly perfused rat intestine-liver preparation. Drug Metab Dispos 18: 580-587.

Hoensch H, Woo CH, Raffin SB and Schmid R (1976) Oxidative metabolism of foreign compounds in rat small intestine: Cellular localization and dependence on dietary iron. Gastroenterology 70: 1063-1070.

Holtbecker N, Fromm MF, Kroemer HK, Ohnhms EF and Heidemann H (1996) The nifedipine-rifampin interaction: Evidence for induction of gut wall metabolism. Drug Metab Dispos 24: 1121-1123.

Ilett KF (1990) In vivo studies of gut wall metabolism, in Clinical Pharmacology and Therapeutics: Presystemic Drug Elimination (George CF, Shand DG andRenwick AG eds) pp 26-53, Butterworths, London.

Ilett KF, Tee LBG, Reeves PT and Minchin RF (1990) Metabolism of drugs and other xenobiotics in the gut lumen wall. Pharmacol Ther 46: 67-93.

Kerremans AL (1996) Cytochrome P450 isoenzymes--importance for the internist. Neth J Med 48(6):237-43.

Kharasch ED, Armstrong AS, Gunn K, Artru A, Cox K, Karol MD (1995) Clinical sevoflurane metabolism and disposition. II. The role of cytochrome P450 2E1 in fluoride and hexafluoroisopropanol formation. Anesthesiology 82(6):1379-88.

Kharasch ED, Thummel KE (1993) Human alfentanil metabolism by cytochrome P450 3A3/4. An explanation for the interindividual variability in alfentanil clearance? Anesth Analg 76(5):1033-9.

Kleinbloesem CH, Van Hartan J, Wilson JPH, Danhof M, Van Brummek P and Breimer DD (1986) Nifedipine: Kinetics and hemodynamic effects in patients with liver cirrhosis after intravenous and oral administration. Clin Pharmacol Ther 40: 21-28.

Klippert P, Borm P and Noordhoek J (1982) Prediction of intestinal first-pass effect of phenacetin in the rat from enzyme kinetic data -Correlation with in vivo data using mucosal blood flow. Biochem Pharmacol 31: 2545-2548.

Klippert PJM, Hulshoff A, Mingels M-JJ, Hofman G and Noordhoek J (1983) Low bioavailability of hexamethylmelamine in the rat due to simultaneous hepatic and intestinal metabolism. Cancer Res 43: 3160-3164.

Klippert PJM and Noordhoek J (1983) Influence of administration route and blood sampling site on the area under the curve: Assessment of gut wall, liver and lung metabolism from a physiological model. Drug Metab Dispos 11: 62-66.

Kolars JC, Benedict P, Schmiedin-Ren P and Watkins PB (1994) Aflatoxin B1-adduct formation in rat and human small bowel. Gastroenterology 106: 433-439.

Kolars JC, Schmiedlin-Ren P, Schuetz JD, Fang C and Watkins PB (1992) Identification of rifampin-inducible P450IIIA4 (CYP3A4) in human small bowel enterocytes. J Clin Invest 90: 1874-1878.

Koop DR (1992) Oxidative and reductive metabolism by cytochrome P450 2E1. FASEB J 6(2):724-30.

Krishna DR and Klotz U (1994) Extrahepatic metabolism of drugs in humans. Clin Pharmacokinet 26: 144-160.

Lampen A, Christians U, Guengerich FP, Watkins PB, Kolars JC, Bader A, Gonschior AK, Dralle H, Hackbarth I and Sewing KF (1995) Metabolism of the immunosuppressant tacrolimus in the small intestine: Cytochrome P450, drug interactions, and interindividual variability. Drug Metab Dispos 23: 1315-1324.

Lieber CS (1997) Cytochrome P-4502E1: its physiological and pathological role. Physiol Rev 77(2):517-44.

Lin JH (1994) Dose-dependent pharmacokinetics: Experimental observations and theoretical considerations. Biopharm Drug Dispos 15: 1-31.

Lin JH, Chiba M, Balani SK, Chen IW, Kwei G, Vastag KJ and Nishime JA (1996) Species-differences in the pharmacokinetics and metabolism of indinavir, a potent human-immunodeficiency-virus protease inhibitor. Drug Metab Dispos 24: 1111-1120.

Lin JH, Chiba M and Baillie TA (1997) In vivo assessment of intestinal metabolism. Drug Metab Dispos 25: 1107-1109.

Lin JH, Chiba M, Baillie TA (1999) Is the role of the small intestine in first-pass metabolism overemphasized? *Pharmacol Rev* 51(2):135-58.

Lipkin M, Sherlock P and Bell B (1963) Cell proliferation kinetics in the gastrointestinal tract of man II. Gastroenterology 45: 721-729.

McKinnon RA, Burgess WM, Hall P, deLa M, Roberts-Thompson SJ, Gonzalez FJ and McManus ME (1995) Characterization of CYP3A gene subfamily expression in human gastrointestinal tissues. Gut 36: 259-267.

Melander A, Danielson K, Hanson DA, Rudell B, Schersten B, Thulin T and Wahlin E (1977a) Enhancement of hydralazine bioavailability by food. Clin Pharmacol Ther 22: 104-107.

Melander A, Danielson K, Scherstein B and Wahlin E (1977b) Enhancement of the bioavailability of propranolol and metoprolol by food. Clin Pharmacol Ther 22: 108-112.

Melander A and McLean A (1983) Influence of food intake on presystemic clearance of drugs. Clin Pharmacokinet 8: 286-296.

Minchin RF and Ilett KF (1982) Presystemic elimination of drugs: Theoretical considerations for quantifying the relative contribution of gut and liver. J Pharm Sci 71: 458-460.

Mistry M and Houston JB (1987) Glucuronidation in vitro and in vivo. Comparison of intestinal and hepatic conjugation of morphine, naloxone and buprenorphine. Drug Metab Dispos 15: 710-717.

Morse MA and Stoner GD (1993) Cancer chemoprevention: principles and prospects. Carcinogenesis (Lond) 14: 1737-1746.

Murray GI, Barnes TS, Swell HF, Ewen SW, Melvin WT and Burk MD (1988) The immunochemical localization and distribution of cytochrome P450 in normal human

hepatic and extrahepatic tissues with a monoclonal antibody to human cytochrome P450. Br J Clin Pharmacol 25: 465-475.

Murray M (1992) P450 enzymes. Inhibition mechanisms, genetic regulation and effects of liver disease. Clin Pharmacokinet 23(2):132-46.

Nelson DR, Koymans L, Kamataki T, Stegeman JJ, Feyereisen R, Waxman DJ, Waterman MR, Gotoh O, Coon MJ, Estabrook RW, Gunsalus IC and Nebert DW (1996) The P450 superfamily, update on new sequences, gene mapping, accession number and nomenclature. Pharmacogenetics 6: 1-42.

Nemeroff CB, DeVane CL, Pollock BG (1996) Newer antidepressants and the cytochrome P450 system. Am J Psychiatry 153(3):311-20.

Oda Y, Furuichi K, Tanaka K, Hiroi T, Imaoka S, Asada A, Fujimori M, Funae Y (1995) Metabolism of a new local anesthetic, ropivacaine, by human hepatic cytochrome P450. Anesthesiology 82(1):214-20.

Olanoff LS, Walle T, Cowart TD, Walle UK, Oexmann MJ and Conradi EC (1986) Food effects on propranolol systemic and oral clearance: Support for a blood flow hypothesis. Clin Pharmacol Ther 40: 408-414.

Pacifici GM, Franchi M and Bencini F (1988) Tissue distribution of drug metabolizing enzymes in human. Xenobiotica 18: 849-856.

Paine MF, Khalighi M., Fisher JM, Shen DD, Kunze KL, March CL, Perkins JD and Thummel KE (1997) Characterization of interintestinal and intraintestinal differences in human CYP3A-dependent metabolism. J Pharmacol Exp Ther 283: 1552-1562.

Paine MF, Shen DD, Kunze KL, Perkins JD, Marsh CL, McVicar JP, Barr DM, Gillies BS and Thummel KE (1996) First-pass metabolism of midazolam by the human intestine. Clin Pharmacol Ther 60: 14-24.

Parks DA and Jacobson ED (1987) Mesenteric circulation, in Physiology of the Gastrointestinal Tract (Johnson LR, Christensen J, Jackson MJ, Jacobson ED and Walsh JH eds) pp 1649-1670, Raven Press, New York.

Peters WH and Kremers PG (1989) Cytochromes P450 in the intestinal mucosa of man. Biochem Pharmacol 38: 1535-1538.

Prueksaritanont T, Dwyer LM and Cribb AE (1995) (+)-Bufuralol 1'-hydroxylation activity in human and rhesus monkey intestine and liver. Biochem Pharmacol 50: 1521-1525.

Renwick AG and George CF (1989) Metabolism of xenobiotics in the gastro-intestinal tract, in Intermediary Xenobiotic Metabolism in Animals: Methodology, Mechanisms and Significance (Huston DH, Caldwell J and Paulson GD eds) pp 13-40, Taylor and Francis, London.

Rowland M, Tozer TN (1995) Genetics. In *Clinical Pharmacokinetics. Concepts and Applications*. Baltimore: Williams and Wilkins, 220-29.

Segel IH (1975) Kinetics of unireactant enzymes, in Enzyme Kinetics (Segel IH ed) pp 18-99, John Wiley and Sons, New York.

Shimada T, Yamazaki H, Mumura M, Inui Y and Guengerich FP (1994) Interindividual variations in human liver cytochrome P450 enzymes involved in the oxidation of drugs, carcinogens and toxic chemicals: Studies with liver microsomes of 30 Japanese and 30 Caucasians. J Pharmacol Exp Ther 270: 414-423.

Shiner M (1995) Anatomy of the small intestine, in Gastroenterology (Haubrich WS ed) vol 5, pp 885-898, WB Saunders Company, Philadelphia.

Shirkey RS, Chakraborty J and Bridges JW (1979) Comparison of the drug metabolizing ability of rat intestinal mucosal microsomes with that of liver. Biochem Pharmacol 28: 2835-2839.

Slaughter RL, Edwards DJ (1995) Recent advances: the cytochrome P450 enzymes. Ann Pharmacother 29(6):619-24.

Sotaniemi EA, Rautio A, Backstrom M, Arvela P, Pelkonen O (1995) CYP3A4 and CYP2A6 activities marked by the metabolism of lignocaine and coumarin in patients with liver and kidney diseases and epileptic patients. Br J Clin Pharmacol 39(1):71-6.

Stadler J, Trockfeld J, Schmalix WA, Brill T, Siewert JR, Greim H, Doehmer J (1994) Inhibition of cytochromes P4501A by nitric oxide. Proc Natl Acad Sci USA 91(9):3559-63.

Strömberg C, Vanakoski J, Olkkola KT, Lindgvist A, Seppäläö T and Laitinen LA (1992) Exercise alters the pharmacokinetics of midazolam. Clin Pharmacol Ther 51: 527-532.

Thomas ABR (1988) Relationship between physiology and clinical disorders of the small intestine, in Principles and Practice of Gastroenterology and Hepatology (Gitnick G, Hollander D, Kaplowitz N, Samloff LM and Schoenfield LJ eds) pp 281-289, Elsevier, Amsterdam.

Thummel KE, Kunze KL and Shen DD (1997) Enzyme-catalyzed process of first-pass hepatic and intestinal drug extraction. Adv Drug Delivery Rev 27: 99-127.

Thummel KE, O'Shea D, Paine MF, Shen DD, Kunze KL, Perkins JD and Wilkinson GR (1995) Oral first-pass elimination of midazolam involves both gastrointestinal and hepatic CYP3A-mediated metabolism. Clin Pharmacol Ther 59: 491-502.

Wang SX, Sutfin TA, Bäärnhielm C and Regardh CG (1989) Contribution of intestine to the first-pass metabolism of felodipine in the rat. J Pharmacol Exp Ther 250: 632-636.

Watkins PB, Wrighton SA, Schuetz EG, Molowa DT and Guzelian PS (1987) Identification of glucocorticoid cytochrome P450 in the intestinal mucosa of rats and man. J Clin Invest 80: 1029-1036.

Weisbradt NW (1987) Motility of the small intestine, in Physiology of the Gastrointestinal Tract (Johnson LR, Christense J, Jackson MJ, Jacobson ED and Walsh JH eds) vol 2, pp 631-663, Raven Press, New York.

Wilkinson GR (1987) Clearance approaches in pharmacology. Pharmacol Rev 39: 1-47.

Wrighton SA, Stevens JC (1992) The human hepatic cytochromes P450 involved in drug metabolism. Crit Rev Toxicol 22(1):1-21.

Wu CY, Benet LZ, Hebert MF, Gupta SK, Rowland M, Gomez DY and Wacher VJ (1995) Differentiation of absorption and first-pass gut and hepatic metabolism in humans: Studies with cyclosporine. Clin Pharmacol Ther 58: 492-497.

Xu X, Hirayama H and Pang KS (1989) First-pass metabolism of salicylamide: Studies in the once-through vascularly perfused rat intestine-liver preparation. Drug Metab Dispos 17: 556-563.

Zhang DY, Wikoff J, Dunbar D, Fasco M and Kaminsky L (1997) Regulation of cytochrome P450 1A1 expression in rat small intestine. Drug Metab Dispos 25: 21-26.